

Chemistry–A European Journal

Supporting Information

Visible-Light Assisted Covalent Surface Functionalization of Reduced Graphene Oxide Nanosheets with Arylazo Sulfones

Lorenzo Lombardi, Alessandro Kovtun, Sebastiano Mantovani, Giulio Bertuzzi,
Laura Favaretto, Cristian Bettini, Vincenzo Palermo, Manuela Melucci,* and Marco Bandini*

Supporting Information

Table of Contents

General methods	S2
General procedure for the synthesis of arylazo mesylates 1	S3
Procedures for the synthesis of aniline precursor 2q and 2r	S7
General procedure for the light promoted functionalization of <i>rGO</i>	S8
XPS characterization of the functionalized 1-rGO materials	S10
XPS of <i>rGO</i> functionalized with chlorine-bearing target molecules	S11
XPS of <i>rGO</i> functionalized with fluorine-bearing target molecules	S12
XPS of <i>rGO</i> functionalized with bromine-bearing target molecules	S13
XPS of <i>rGO</i> functionalized with pyridine and thiophene-bearing target molecules	S14
XPS of <i>rGO</i> functionalized with iodine-bearing target molecules	S15
XPS characterization of the functionalized 1-GO	S16
Procedure for the Suzuki coupling on functionalized 1m-rGO	S18
XPS binding energies and C 1s fits	S19
Raman characterization of the functionalized 1a-HOPG	S23
Absorption spectra	S25
NMR Spectra of new compounds	S33
References	S42

General Methods

NMR spectra were recorded with a Varian Mercury 400 spectrometer (400 MHz for ^1H -NMR and 100 MHz for ^{13}C -NMR spectra) and Agilent NMR spectrometer 500 MHz (500 MHz for ^1H -NMR, 470.322 MHz for ^{19}F -NMR and 125 MHz for ^{13}C -NMR spectra).

The chemical shifts (δ) are reported in ppm (parts per million) referred to the signals of the residual solvents (^1H CHCl_3 = 7.26 ppm and DMSO = 2.48 ppm; ^{13}C CHCl_3 = 77.0 ppm and DMSO = 40.0 ppm).

Coupling constants (J) are reported in Hz and multiplicity are named by the following abbreviations: singlet (s), doublet (d), doublet of doublets (dd), triplet (t), quartet (q), multiplet (m), broad (b) and impurity or residual solvent (*).

MS spectra were taken by electron impact (EI) ionization at 70 eV on a Trace 1300 GC, ISQ Single Quadrupole MS, Thermo Fisher Scientific and the sample was introduced to the ion source region via a direct exposure probe (DEP); they are reported m/z and relative intensity of main fragments. ATR FT-IR spectra were recorded with Agilent Cary 630 FTIR spectrophotometer and the spectra are expressed by wavenumber (cm^{-1}).

Commercially available chemicals were purchased from Sigma Aldrich and Fluorochem and used without any further purification; Reduced Graphene Oxide (*rGO*) partly reduced with Carbon content of about 85% atomic in powder was purchased from Abalonyx, chromatographic purification was done with 40-63 μm Merck (Geduran) silica gel.

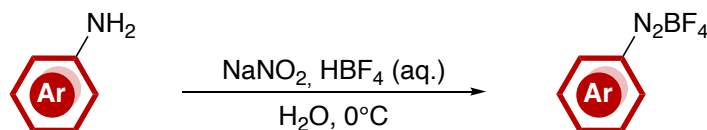
XPS spectra were acquired by using a Phoibos 100 hemispherical energy analyzer (Specs) using Mg K_α radiation ($\hbar\omega$ = 1253.6 eV). The X-ray power was 125 W. The spectra were recorded in the constant analyser energy (CAE) mode with analyser pass energies of 10 eV for the high-resolution spectra. Charging effects were corrected by energy calibration on C 1s at 284.6 eV. Overall resolution of 0.9 eV was determined on Ag $3d_{5/2}$. The base pressure in the analysis chamber during analysis was 5×10^{-9} mbar. High resolution XPS spectra of C 1s were analysed by CasaXPS (Casa software, Ltd), the curve fitting was carried out using Gaussian/Lorentzian curves shape (GL(30)) for C-O groups with a full width half-maximum of 1.4 eV and an asymmetric Voigt for the C-C sp^2 . Shirley background was subtracted prior the fit. The C 1s signal was fitted only in case of pristine *rGO* and GO, revealing the relative amounts of functional groups:¹ aromatic carbon (C-C sp^2 , 284.4 eV), aliphatic carbon (C-C sp^3 , 285.0 eV), hydroxyl (C-OH, 285.7 eV), epoxy (C-O-C, 286.7 eV), carbonyl (C=O, 288.0 eV), carboxyl (O-C=O, 289.1 eV) and aromatic carbons near vacancies (C-C* sp^2 , 283.5).² More detail on consistency of the fitting procedure are reported in our previous work on C 1s fit.¹ In case of aryl functionalized *rGO* or GO the C 1s was directly compared by subtracting the correspondent reference sample in order to underline the signal differences. GO was measured as a dry powder deposited on conductive carbon tape.

Raman spectroscopy was performed by LabRam instrument (Jobin Yvon). He-Ne laser excitation and Olympus BX 40 microscope with 100x objective (632.1 nm) were used. The spot size of laser was about 1 μm and for each sample 8 different spot were measured and results mediated.

General procedure for the synthesis of Arylazo mesylates **1**

All compounds were prepared from the corresponding anilines via a two-steps sequence involving the formation of the aryldiazonium tetrafluoroborate salt and its subsequent conversion to the target compound by addition of sodium methanesulfinate.

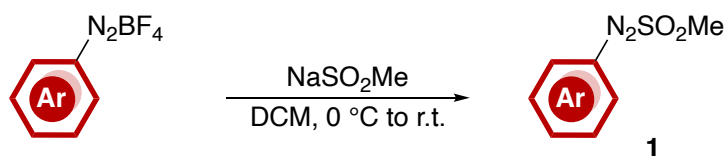
Aryldiazonium tetrafluoroborate salts were prepared via a slight modification of a known procedure.³



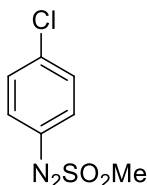
The appropriate aniline (10 mmol) was dissolved in a mixture of 4 mL of deionized H₂O and 3.4 mL of 48 wt. % aqueous HBF₄. (For 3-aminopyridine, precursor for compound **10**, EtOH was used instead of H₂O in the whole procedure).

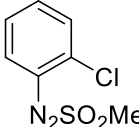
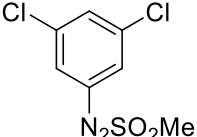
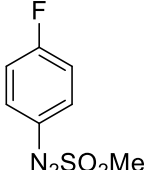
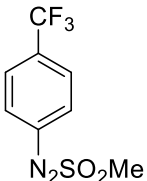
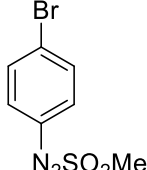
After cooling the reaction mixture to 0 °C, NaNO₂ (10 mmol, 690 mg in 2 mL of H₂O) was added dropwise in 5 min. The resulting mixture was stirred at 0 °C for 45 min and the precipitate was collected by filtration, washed with cold H₂O, diethyl ether and dried under vacuum to yield aryldiazonium tetrafluoroborate salt in 50-90% yield.

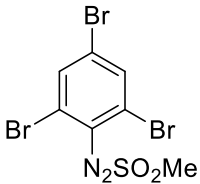
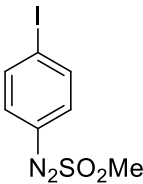
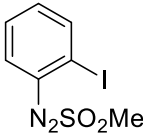
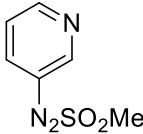
Diazonium salts were converted to the arylazo mesylates **1** via the procedure described by Protti *et al.*⁴

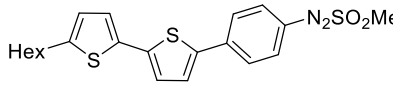
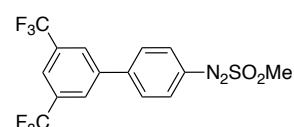


To a cooled (0 °C) suspension of the appropriate aryldiazonium salt (5 mmol, 1 eq) in 10 mL of DCM was added NaSO₂Me (5 mmol, 514.5 mg, 1 eq) in one portion. The temperature was allowed to rise to room temperature and the solution stirred overnight. The resulting mixture was then filtered, and the obtained solution evaporated. The raw solid was purified by dissolution in cold DCM and precipitation by adding *n*-hexane.

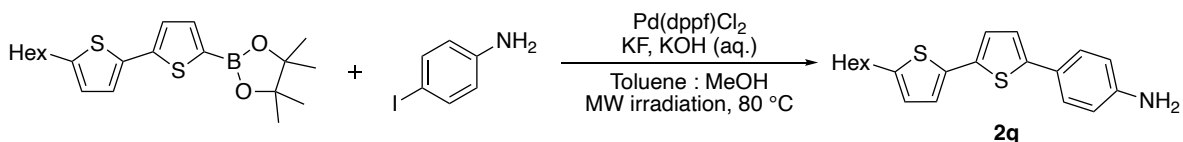
 <chem>Clc1ccc(cc1)N=[N+]c2ccccc2.S(=O)(=O)C</chem>	1a. Pale yellow solid; yield = 92%. Spectral data match those reported in the literature. ⁵
 <chem>Clc1cccc(c1)N=[N+]c2ccccc2.S(=O)(=O)C</chem>	1b. Orange solid; yield = 69%. Spectral data match those reported in the literature. ⁶

	<p>1c. Yellow-orange solid; yield = 77%. Spectral data match those reported in the literature.⁶</p>
	<p>1d. Yellow solid; yield = 48%. Spectral data match those reported in the literature.⁵</p>
	<p>1e. Yellow solid; yield = 51%. Spectral data match those reported in the literature.⁵</p>
	<p>1f. Yellow solid; yield = 76%. Spectral data match those reported in the literature.⁵</p>
	<p>1g. Yellow solid; yield = 71%. Spectral data match those reported in the literature.⁵</p>
	<p>1h. Orange solid (<i>m.p.</i> = decomposition above 120 °C); yield = 74%. ¹H-NMR (400 MHz, CDCl₃) δ ppm: 8.41 (s, 2H), 8.17 (s, 1H), 3.30 (s, 3H) ¹³C-NMR (100 MHz, CDCl₃) δ ppm: 149.3, 133.7 (q, <i>J</i> = 34.3Hz), 127.7 (m), 124.3 (d, <i>J</i> = 3.8Hz), 122.4 (q, <i>J</i> = 272.3Hz), 35.2. ¹⁹F-NMR (470.322 MHz, CDCl₃) δ ppm: -63.11. ATR FT-IR: 3218, 3086, 3024, 1610, 1500, 1462, 1331, 1276, 1193, 1127. MS-DEP (m/z): 241.0 (16%), 213.0 (100%), 163.0 (17%).</p>
	<p>1i. Yellow solid; yield = 85%. Spectral data match those reported in the literature.^[5]</p>
	<p>1j. Orange solid; yield = 55%. Spectral data match those reported in the literature.⁵</p>

	<p>1k. Yellow solid; yield = 78%. Spectral data match those reported in the literature.⁷</p>
	<p>1l. Orange solid (<i>m.p.</i> = decomposition above 120 °C); yield = 60%. ¹H-NMR (400 MHz, DMSO-<i>d</i>₆) δ ppm: 8.22 (s, 2H), 3.48 (s, 3H). ¹³C-NMR (100 MHz, DMSO<i>d</i>₆) δ ppm: 144.4, 136.6, 126.1, 117.4, 35.5. ATR FT-IR: 3102, 3069, 3040, 2933, 1558, 1536, 1496, 1327, 1154. MS-DEP (<i>m/z</i>): 391.6 (4%), 340.6 (52%), 312.6 (100%), 234.78 (46%), 154.88 (25%).</p>
	<p>1m. Orange solid; yield = 93%. Spectral data match those reported in the literature.^[8]</p>
	<p>1n. Ocher solid (<i>m.p.</i> = decomposition above 120 °C); yield = 50%. ¹H-NMR (400 MHz, DMSO-<i>d</i>₆) δ ppm : 8.2 (dd, <i>J</i> = 7.6Hz, <i>J</i> = 1.2Hz, 1H), 7.65 - 7.57 (m, 2H), 7.48 (m, 1H), 3.44 (s, 3H). ¹³C-NMR (100 MHz, DMSO-<i>d</i>₆) δ ppm : 148.6, 141.2, 137.2, 130.3, 118.1, 106.1, 35.5. ATR FT-IR: 3020, 1570, 1478, 1456, 1321, 1257, 1154. MS-DEP (<i>m/z</i>): 230.9 (28%), 202.9 (100%), 76.0 (41%).</p>
	<p>1o. Pale orange solid; yield = 15%. Spectral data match those reported in the literature.⁵</p>
	<p>1p. Orange solid (<i>m.p.</i> = decomposition above 120 °C); yield = 70%. ¹H-NMR (400 MHz, DMSO-<i>d</i>₆) δ ppm: 7.76 (d, <i>J</i> = 1.2Hz, 1H), 3.83 (s, 3H), 3.34 (s, 3H), 2.26 (d, <i>J</i> = 1.2Hz, 3H). ¹³C-NMR (100 MHz, DMSO-<i>d</i>₆) δ ppm: 160.8, 148.8, 134.4, 131.3, 129.9, 53.4, 34.6, 16.2. ATR FT-IR: 3114, 3023, 2933, 1738, 1703, 1437, 1316, 1291, 1239, 1154. MS-DEP (<i>m/z</i>): 233.9 (24%), 201.9 (56%), 183.0 (69%), 139.9 (100%), 125.0 (65%).</p>

	<p>1q. Dark red solid (<i>m.p.</i> = decomposition above 120 °C); yield = 76%. ¹H-NMR (400 MHz, DMSO-<i>d</i>₆) δ ppm : 7.96 (dd, <i>J</i>=8.4Hz, <i>J</i>=2.4Hz, 2H), 7.76 (dd, <i>J</i>=8.4Hz, <i>J</i> = 2.0Hz, 2H), 7.42 (d, <i>J</i>=4.0Hz, 1H), 7.13 (d, <i>J</i> = 4.0 Hz, 1H), 7.08 (d, <i>J</i> = 3.6Hz, 1H), 6.73 (d, <i>J</i>=3.6Hz, 1H), 3.23 (s, 3H), 2.82 (t, <i>J</i> = 7.6Hz, 2H), 1.74 – 1.66 (m, 2H), 1.42 – 1.28 (m, 6H), 0.92 (m, 3H). ¹³C-NMR (100 MHz, CDCl₃) δ ppm : 147.6, 146.8, 141.0, 140.6, 139.8, 134.0, 126.6, 125.9, 125.7, 125.1, 124.3, 124.3, 34.9, 31.5 (2C), 30.2, 28.7, 22.6, 14.1 ATR FT-IR: 2922, 2850, 1727, 1591, 1499, 1457, 1435, 1336, 1311, 1141 MS-DEP (<i>m/z</i>): 340.9 (20%), 269.9 (20%), 207.0 (100%)</p>
	<p>1r. Yellow-orange solid (<i>m.p.</i> = decomposition above 120 °C); yield = 48%. ¹H-NMR (400 MHz, CDCl₃) δ ppm: 8.12 – 8.07 (m, 4H), 7.96 (bs, 1H), 7.84 (d, <i>J</i>=9.2 Hz, 2H), 3.27 (s, 3H). ¹³C-NMR (125 MHz, CDCl₃) δ ppm: 148.9, 144.5, 141.3, 132.6 (q, <i>J</i>= 33.3 Hz), 128.6, 127.4 (m), 125.4, 123.1 (q, <i>J</i> = 271.3 Hz), 122.3 (m), 34.9. ¹⁹F-NMR (470.322 MHz, CDCl₃) δ ppm : -62.9. ATR FT-IR: 1602, 1472, 1373, 1338, 1275, 1121. MS-DEP (<i>m/z</i>): 151.99 (25%), 201.00 (35%), 221.04 (15%), 289.96 (100%).</p>

Procedures for the synthesis of aniline precursors **2q** and **2r**



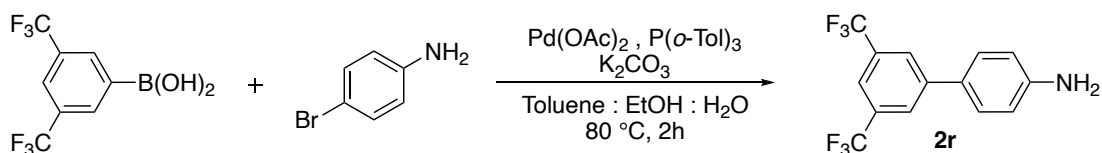
4-Iodoaniline (0.9 mmol, 197 mg, 1 eq), 2-(5'-hexyl-[2,2'-bithiophen]-5-yl)-4,4,5,5-tetramethyl-1,3,2-dioxaborolane (0.95 mmol, 357 mg, 1.05 eq), KF (7.2 mmol, 420 mg, 8 eq) and [1,1'-bis(diphenylphosphino)ferrocene]dichloropalladium(II) complex with dichloromethane (0.09 mmol, 70 mg, 10 mol%) were added to a mixture of 5 ml KOH aqueous saturated solution, 10 ml toluene and 10 ml methanol. The reaction mixture was irradiated for 45 minutes at 80 °C (power max 200 watt) in a microwave reactor (CEM, Discover-SP; MAG. FREQ. 2455 MHz).

After completion, the organic layer was separated, the aqueous layer was extracted with DCM x 2 and the combined organic layers were washed with water.

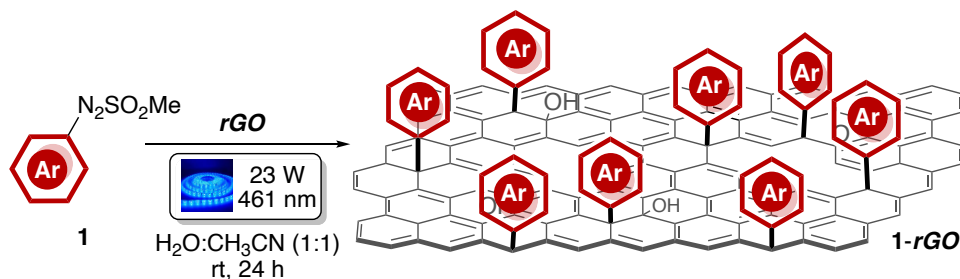
The combined organic layers were dried over Na₂SO₄, the solvent was evaporated and the residue was purified by silica gel flash chromatography (*n*-pentane: EtOAc 95:5 -> 80:20). Finally, the collected product was crystallized from toluene and cold pentane to yield **2q** as brown solid.

	<p>2q. Light brown solid (<i>m.p.</i> = 142 - 146 °C); yield 75%. ¹H-NMR (400 MHz, Acetone-d₆) δ ppm: 7.40 – 7.35 (m; 2H), 7.11 (d, <i>J</i>=3.6Hz; 1H), 7.08 (d, <i>J</i>=3.6Hz; 1H), 7.02 (d, <i>J</i>=3.6Hz; 1H), 6.76 (d, <i>J</i>=3.6Hz; 1H), 6.72 – 6.67 (m, 2H), 4.86 (br; 1H), 2.84 – 2.77 (m; 2H), 1.72 – 1.63 (m; 2H), 1.42 – 1.23 (m; 6H), 0.89 (t, <i>J</i>= 6.8Hz; 3H). ¹³C-NMR (100 MHz, Acetone-d₆) δ ppm: 148.5, 144.5, 143.9, 135.0, 134.3, 132.6, 126.4, 125.1, 123.8, 122.7, 121.1, 114.4, 31.5, 31.4, 29.5, 28.5, 22.3, 13.4. ATR FT-IR: 3424, 3384, 3300, 3197, 2922, 2854, 1623, 1603, 1507, 1451, 1269, 1181. MS-DEP (<i>m/z</i>): 341.0 (28%); 269.9 (100%).</p>
--	---

Aniline **2r**, precursor for compound **1r**, was synthesized via Suzuki coupling between 3,5-bis(trifluoromethyl)phenyl boronic acid and 4-bromoaniline, according to a known procedure.⁹ Spectral data match those reported in the literature.



General procedure for the light promoted functionalization of *rGO*



A 20 mL screw-capped vial was charged with arylazo mesylate **1** (0.5 mmol), *rGO* powder (30 mg), 5 mL H_2O and 5 mL CH_3CN . The reaction vessel was sealed and stirred under blue light irradiation (Blue LED stripe, 461 nm, 23 W, distance about 10 cm) at room temperature for 24 hours.

The mixture was then filtered on a paper filter and the solid was washed with DCM until the washings become colorless, followed by MeOH, H_2O and acetone. The solid was collected and dried under vacuum to yield functionalized **1-rGO**. (32.5 – 41.1 mg, see Table S1 below).

Table S1. Quantity of recovered functionalized **1-rGO** for each substrate and corresponding aryl content (atomic %, XPS).

Entry	Ar (1)	Aryl [%] content	Recovered material (mg)
1	4-Cl(C_6H_4) (1a)	34 ± 3	37.0
2	3-Cl(C_6H_4) (1b)	38 ± 4	38.4
3	2-Cl(C_6H_4) (1c)	37 ± 5	38.2
4	3,5-Cl ₂ (C_6H_3) (1d)	33 ± 3	37.9
5	3-F(C_6H_4) (1e)	31 ± 3	38.8
6	4-F(C_6H_4) (1f)	21 ± 3	40.4
7	4-CF ₃ (C_6H_4) (1g)	31 ± 3	38.4
8	3,5-(CF ₃) ₂ (C_6H_3) (1h)	26 ± 3	36.4
9	4-Br(C_6H_4) (1i)	40 ± 4	40.8
10	3-Br(C_6H_4) (1j)	31 ± 3	38.0
11	2-Br(C_6H_4) (1k)	37 ± 4	38.4
12	2,4,6-Br ₃ (C_6H_2) (1l)	15 ± 2	35.9
13	4-I(C_6H_4) (1m)	24 ± 3	41.1
14	2-I(C_6H_4) (1n)	10 ± 2	36.5
15	3-pyridyl (1o)	23 ± 3	32.5
16	1p	13 ± 2	35.8
17	1q	76 ± 4	41.0
18	1r	45 ± 4	40.8

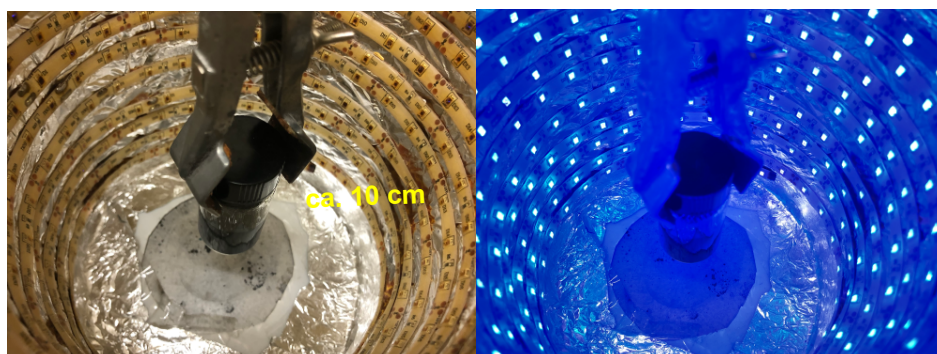


Figure S1. Experimental set-up of the “photochemical-well” with LEDs off (left) and on (right).

XPS characterization of the functionalized 1-*rGO* materials

In order to evaluate the functionalization degree of all molecules covalently grafted to *rGO* we used a quantitative parameter named “aryl functionalization”, that was directly obtained from the stoichiometry of each molecule. The ratio between the overall number of atoms (except H, that is not detectable by XPS) that compose each molecule, divided by the number of target atoms (i.e. Cl, F, Br, I, N, S) can be used for calculate the overall “aryl content”:

$$\text{aryl content (\%)} = \text{Target XPS concent (at.\%)} \cdot \frac{\text{total atom in target molecule}}{\text{target atoms}}$$

By using this parameter, we were able to compare the functionalization degree of extremely different molecules, i.e. **1e** and **1h**, that have quite different amounts of F: 3 and 11 % respectively, but the ratio presents a comparable aryl functionalization of 21 and 26 %, respectively.

Moreover, these values can be confirmed by XPS C 1s analysis: the C atom corresponding to C-F₃ bond in **1g-rGO** and **1h-rGO** present a univocally associated chemical shift respect to the main C 1s signal (Aromatic carbon) of +7.6 eV. The aryl functionalization can be further calculated by using the same stoichiometric considerations on C-F₃ relative abundance on C 1s:

$$\text{C 1s aryl content (\%)} = \text{C} - \text{F}_3(\%) \cdot \frac{\text{total atom in } \mathbf{1g}}{\text{C atoms bonded F}}$$

XPS of *rGO* functionalized with Chlorine-bearing target molecules

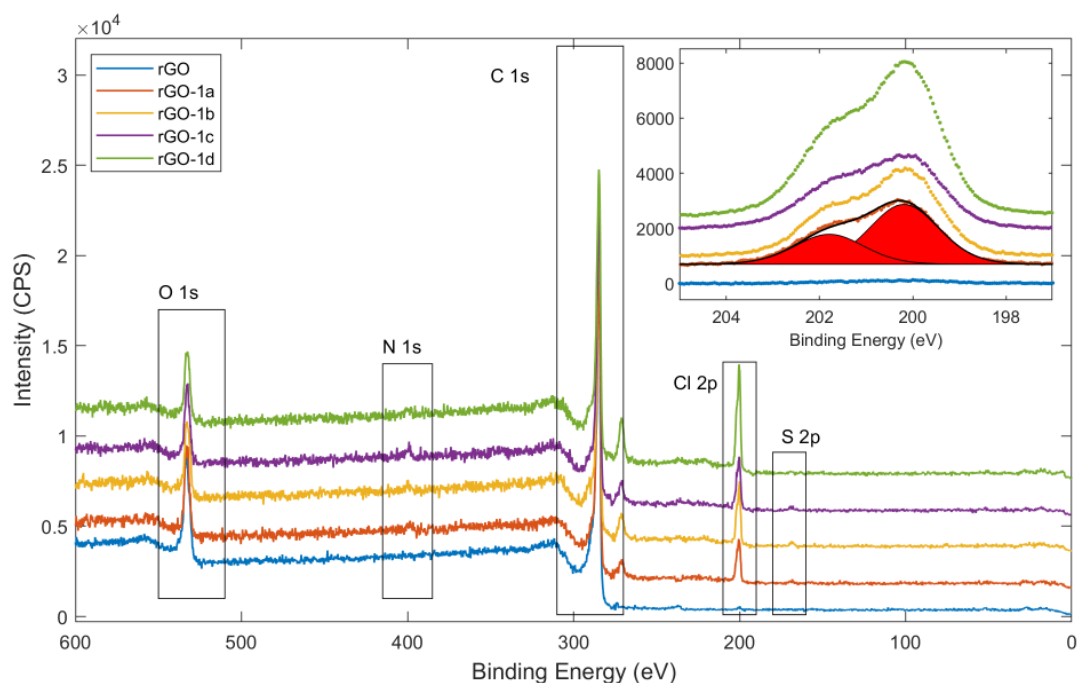


Figure S2. XPS survey spectra of covalently grafted *rGO* by molecules containing Cl: **1a** (orange), **1b** (yellow), **1c** (purple) and **1d** (green). O 1s, N 1s, C 1s, Cl 2p and S 2p signals are present. Inset: high resolution Cl 2p signal fitted by doublet.

Table S2. Chemical composition and overall aryl content of target molecules containing Cl.

Entry	Ar (1)	aryl [%] content	Cl (%)	O/C	N (%)	S(%)
1	4-Cl(C ₆ H ₄) (1a)	34 ± 3	4.8 ± 0.3	0.16 ± 0.01	0.8 ± 0.1	0.4 ± 0.1
2	3-Cl(C ₆ H ₄) (1b)	38 ± 4	6.3 ± 0.4	0.14 ± 0.01	0.9 ± 0.1	0.5 ± 0.1
3	2-Cl(C ₆ H ₄) (1c)	37 ± 4	6.2 ± 0.5	0.14 ± 0.01	1.3 ± 0.2	0.5 ± 0.1
4	3,5-Cl ₂ (C ₆ H ₃) (1d)	33 ± 3	11.1 ± 0.8	0.14 ± 0.01	0.5 ± 0.1	0.2 ± 0.1

XPS of *rGO* functionalized with Fluorine-bearing target molecules

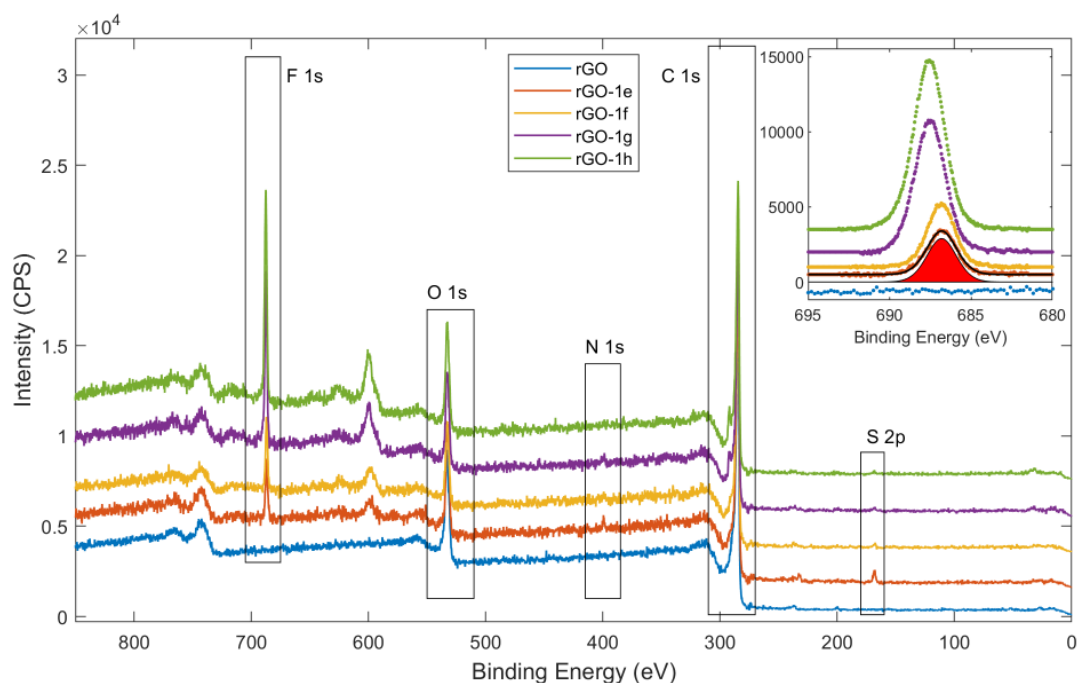


Figure S3. XPS survey spectra of covalently grafted *rGO* by molecules containing F: **1e** (orange), **1f** (yellow), **1g** (purple) and **1h** (green). F 1s, O 1s, N 1s, C 1s, and S 2p signals are present. Inset: high resolution F 1s signal fitted by single component.

Table S3. Chemical composition and overall aryl content of target molecules containing F.

Entry	Ar (1)	Aryl [%] content	F (%)	O/C	Cl (%)	N (%)	S(%)
1	3-F(C ₆ H ₄) (1e)	21 ±3	3.0 ±0.3	0.16 ± 0.01	0.1 ± 0.1	0.5 ±0.1	1.5 ±0.1
2	4-F(C ₆ H ₄) (1f)	31 ±3	4.4 ±0.3	0.16 ± 0.01	0.1 ± 0.05	0.9 ±0.1	0.4 ±0.1
3	4-CF ₃ (C ₆ H ₄) (1g)	31 ±3 ^a	9.3 ±0.5	0.15 ± 0.01	0.2 ± 0.1	0.9±0.1	0.5 ±0.1
4	3,5-(CF ₃) ₂ (C ₆ H ₃) (1h)	26 ±3 ^a	11.0 ±0.8	0.16 ± 0.01	0.1 ± 0.05	0.5 ±0.1	0.3 ±0.1

^a Overall aryl content confirmed by C 1s analysis for molecules **1g** (28%) and **1h** (19%).

XPS of *rGO* functionalized with Bromine-bearing target molecules

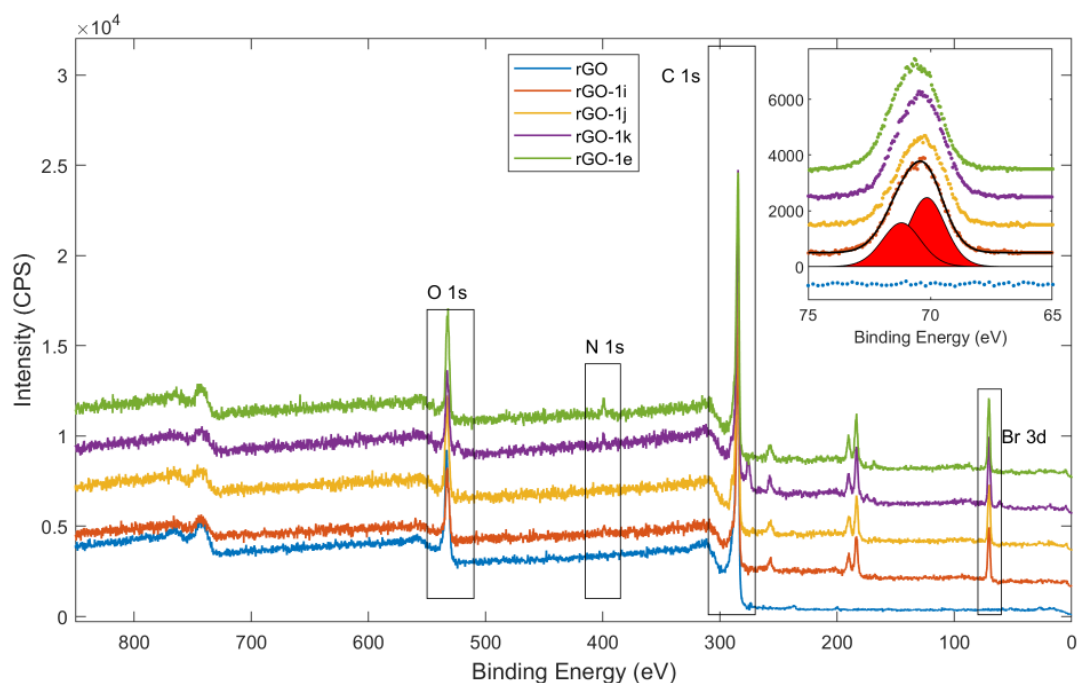


Figure S4. XPS survey spectra of covalently grafted *rGO* by molecules containing Br: **1i** (orange), **1j** (yellow), **1k** (purple) and **1e** (green). O 1s, N 1s, C 1s, and Br 3d signals are present. Inset: high resolution Br 3d signal fitted by doublet.

Table S4. Chemical composition and overall aryl content of target molecules containing Br.

Entry	Ar (1)	Aryl [%] content	Br (%)	O/C	Cl (%)	N (%)	S(%)
1	4-Br(C ₆ H ₄) (1i)	40 ±4	5.8 ±0.4	0.14±0.01	0.2± 0.1	1.1 ±0.1	0.4 ±0.1
2	3-Br(C ₆ H ₄) (1j)	31 ±3	4.4 ±0.3	0.17±0.01	0.2± 0.1	0.9 ±0.1	0.4 ±0.1
3	2-Br(C ₆ H ₄) (1k)	37 ±4	5.3 ±0.5	0.13±0.01	0.2± 0.1	1.4 ±0.2	0.4 ±0.1
4	2,4,6-Br ₃ (C ₆ H ₂) (1l)	15 ±2	5.1 ±0.4	0.19±0.01	0.2± 0.1	2.2 ±0.3	0.4 ±0.1

XPS of *rGO* functionalized with Pyridine and thiophene-bearing target molecules

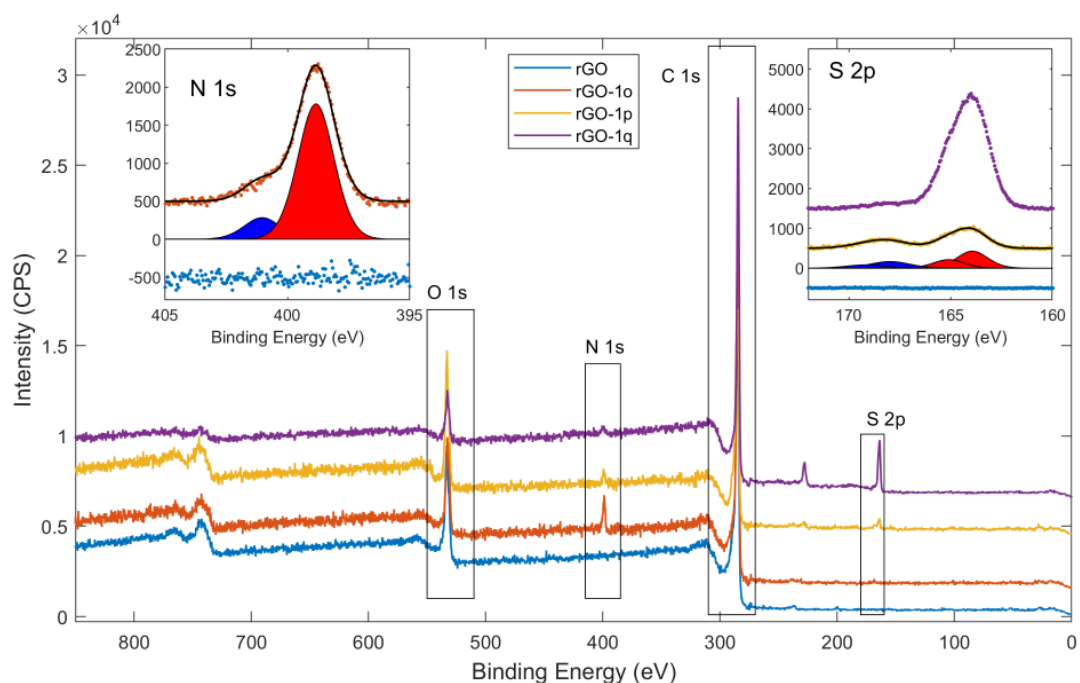


Figure S5. XPS survey spectra of covalently grafted *rGO* by molecules containing pyridine N, **1o** (orange) and thionyl S **1p** (yellow) and **1q** (purple). O 1s, N 1s, C 1s, and S 2p signals are present. Insets: high resolution N 1s and S 2p signals.

Table S5. Chemical composition and overall aryl content of target molecules containing pyridine N and thiophene S.

Entry	Ar (1)	Aryl [%] content	S 2p (%) C-S-C	O/C	Cl (%)	N (%)	S (%) S-O ₂
1	3-pyridyl (1o)	23 ± 3	-	0.15±0.01	0.2 ± 0.1	3.9 ± 0.1	0.4 ± 0.1
2	1p	13 ± 2	1.3 ± 0.2	0.24±0.01	0.1 ± 0.05	2.0 ± 0.3	0.7 ± 0.1
3	1q	76 ± 4	6.9 ± 0.4	0.07±0.01	<0.1	1.2±0.1	0.4 ± 0.1

XPS of *rGO* functionalized with Iodine-bearing target molecules.

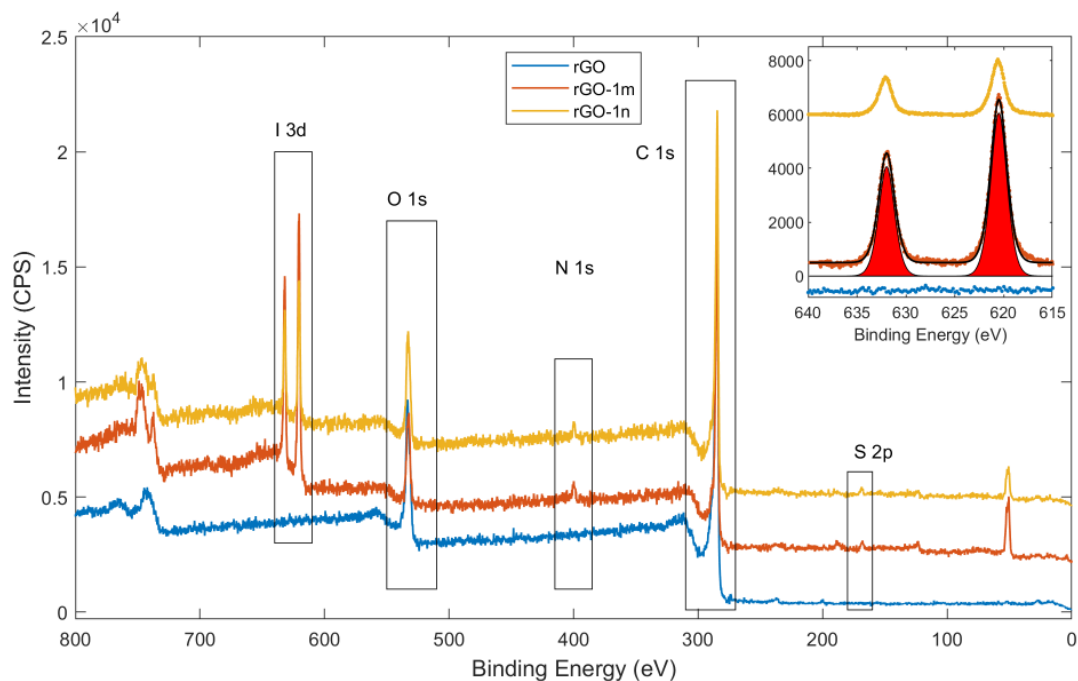


Figure S6. XPS survey spectra of covalently grafted *rGO* by molecules containing I: **1m** (orange), **1n** (yellow). O 1s, N 1s, C 1s, and I 3d signals are present. Inset: high resolution I 3d signal fitted by doublet.

Table S6. Chemical composition and overall aryl content of target molecules containing I.

Entry	Ar (1)	aryl [%] content	I (%)	F 1s	O/C	Cl (%)	N (%)	S(%)
1	4-I(C ₆ H ₄) (1m)	24 ± 3	3.4±0.3	-	0.17±0.01	0.1 ± 0.05	2.6 ± 0.3	1.0 ± 0.1
2	2-I(C ₆ H ₄) (1n)	10 ± 2	1.5±0.2	-	0.17±0.01	0.2 ± 0.1	2.0 ± 0.1	0.7 ± 0.1

XPS characterization of the functionalized 1-GO materials

The covalent grafting of **1a** and **1g** was attempted on GO with the same procedure used for *rGO*, the results are reported in Table S7. The functionalization degree was remarkably lower respect to *rGO* due to the lower abundance of sp² aromatic carbon on GO (about 50%). Moreover, GO is less stable in reaction conditions. Reduction of the material is observed upon irradiation with Blue LED light: the O/C ratio decreases from 0.40 in pristine GO down to 0.32 after irradiation. Reduction is observed as well in the control reaction run in the dark with GO and **1a**: the O/C ratio in this case decreases to 0.27.

GO, differently from *rGO*, presents Cl, N and S atoms within its structure (in amount lower than 1%), thus the variations of N and S are less informative about the incorporation of N and S containing fragments. In case of substrate **1a** the control reaction in the dark shows a Cl content of 0.7 %, identical to the pristine GO content, while irradiation increases the Cl content up to 1.4%. For substrate **1g** we observe a similar behaviour: GO+**1g** in the dark shows 1.9% F, while under LED irradiation the F content increases up to 2.7%. In both cases the overall aryl content is similar (c.a. 10%).

Table S7. Chemical composition and overall aryl content of target molecules containing Cl and F on GO.

Entry	Description	Aryl [%] content	F (%)	O/C	Cl (%)	N (%)	S(%)
1	Pristine GO	-	-	0.40±0.01	0.8 ± 0.1	0.9±0.1	0.3 ±0.1
2	GO + Blue LED 23W (461nm) ^a	-	-	0.32±0.01	0.5 ±0.3	0.8±0.1	0.4 ±0.1
3	GO + 1a ^[b]	5 ± 1	-	0.27±0.01	0.7 ± 0.1	1.2± 0.1	0.5± 0.1
4	GO + 1a + Blue LED 23W (461nm)	10 ± 1	-	0.28±0.01	1.4 ± 0.1	1.2± 0.1	0.3± 0.1
5	GO + 1g ^b	6 ± 1	1.9 ± 0.3	0.39 ±0.01	0.5 ± 0.1	0.7± 0.1	1.3± 0.1
6	GO + 1g + Blue LED 23W (461nm)	9 ± 1	2.7 ± 0.3	0.35 ±0.01	0.3 ± 0.1	0.8± 0.1	0.4± 0.1

^aAbsence of **1a** or **1g**. ^b Absence of LED illumination.

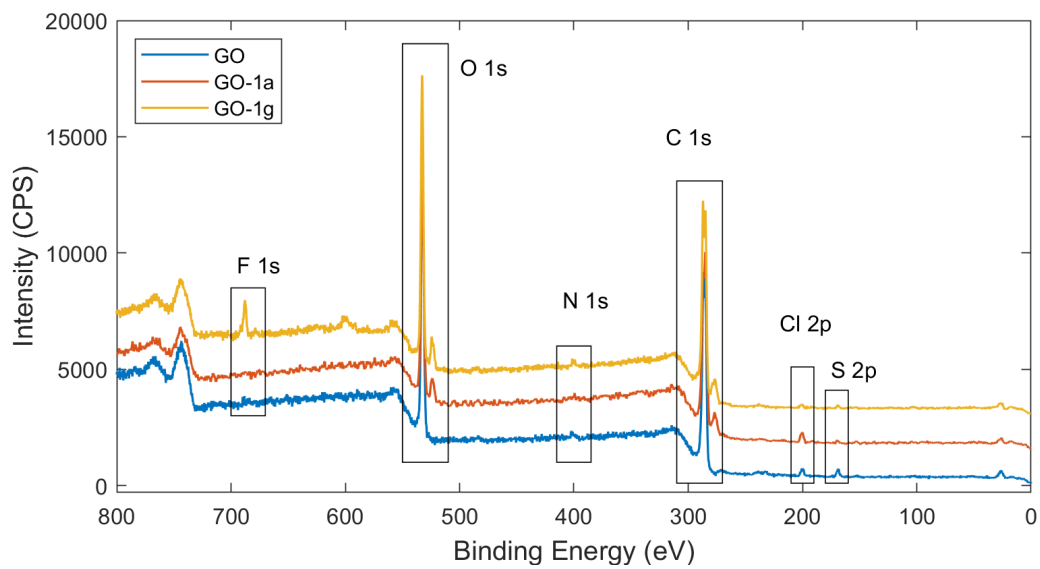
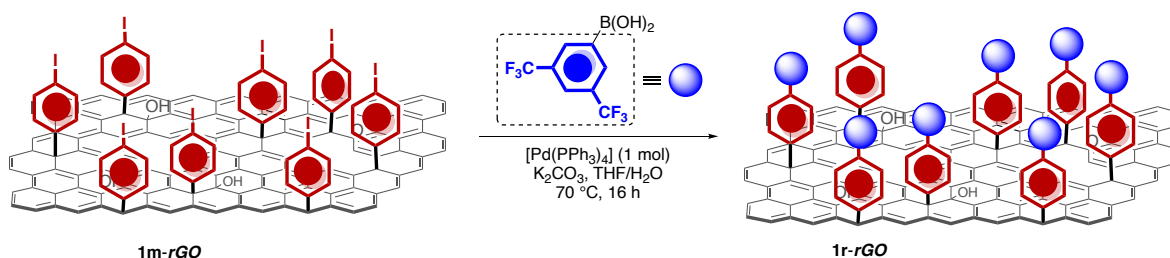


Figure S7. XPS survey spectra of covalently grafted GO by molecules containing Cl (**1a**) and F (**1g**).

Procedure for the Suzuki coupling on functionalized **1m-rGO**.



A dry Schlenk tube was charged with functionalized material **1m-rGO** (20 mg), K_2CO_3 (138 mg, 1 mmol, 1.2 eq), 3,5-Bis(trifluoromethyl)phenylboronic acid (103.2 mg, 0.4 mmol, 1 eq), $\text{Pd(PPh}_3\text{)}_4$ (4.6 mg, 0.004 mmol, 1 mol%), THF (1 mL) and H_2O (0.5 mL). The mixture was stirred overnight at 70°C and then diluted with MeOH. The mixture was centrifuged, the supernatant was discarded and MeOH (5 mL) was added. Centrifugation was repeated 3 times washing with MeOH and 2 times washing with H_2O . Finally, the solid was collected, washed with MeOH and dried under vacuum to yield functionalized material **1r-rGO**.

Table S8. Chemical composition and overall aryl content of **1r-rGO** prepared by both Path a (substitution of I on material **1m-rGO** via Suzuki coupling described above) and path b (via light promoted functionalisation with **1r** according to general procedure).

Entry	Ar (1)	aryl [%] content	I (%)	F 1s	O/C	Cl (%)	N (%)	S(%)
1	1r (path a)	F = 16 ± 2 I = 4 ± 1	0.5 ± 0.1	6.7 ± 0.4	0.15 ± 0.01	<0.1	1.5 ± 0.2	0.6 ± 0.1
2	1r (path b)	F = 45 ± 4	-	13.5 ± 0.5	0.11 ± 0.01	0.10 ± 0.05	0.7 ± 0.1	0.2 ± 0.1

XPS Binding Energies and C 1s fits

All spectra were calibrated to C 1s at 284.6 eV, absolute error on Binding Energy was $\pm 0.1/\pm 0.2$ eV. Reference values taken from literature were adjusted to B.E. of C 1s at 284.6 eV. C 1s is usually fitted by several components corresponding to C-C and C-O bonds, but in the presence of heteroatoms such as halogens, nitrogen and sulphur in significant amount, the fit model would require too many components, many of those in uncertain position, thus we decided to plot the C 1s and the difference of the grafted *rGO* and the pristine one. Some features emerged from this plot as effective peaks, particularly evident in case of **1g-rGO**, where the chemical shift was +7.6 eV, in excellent agreement with literature. In all other cases the peak corresponding to C-heteroatom bond was found closer to sp^2 aromatic carbon (chemical shifts in order of 1-2 eV).

Table S9. Binding Energies of *rGO* functionalised by target molecules containing Cl. Cl 2p 3/2 value with C 1s calibration at 284.6 eV.

Entry	Ar (1)	Target atom reference	C 1s	O 1s	Cl 2p	N 1s	S 2p _{3/2}
1	<i>rGO</i> pristine		284.6	538.8	199.8	-	-
2	4-Cl(C ₆ H ₄) (1a)		285.6	532.8	200.2	399.4	168.4
3	3-Cl(C ₆ H ₄) (1b)			532.6	200.1	399.3	168.3
4	2-Cl(C ₆ H ₄) (1c)			532.7	200.2	399.3	168.3
5	3,5-Cl ₂ (C ₆ H ₃) (1d)		285.6	532.7	200.1	399.4	168.4
6		N-SO ₂ -C ^[10]					168.1- 168.8
7		C-N=N-C ^[11]	284.6			399.4	
8		C ₆ H ₅ -Cl ^[12]			200.1*		

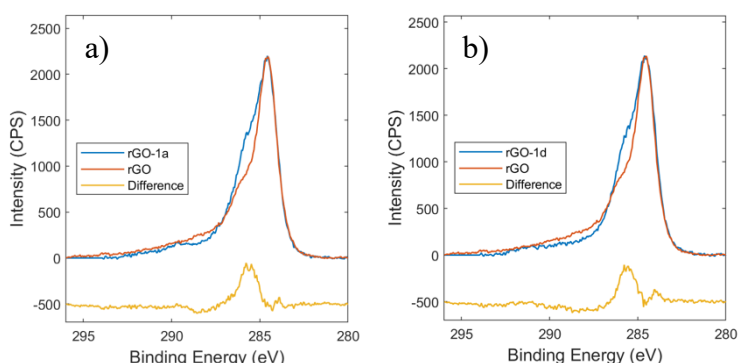


Figure S8. XPS C1s spectra of covalently grafted *rGO* by molecules containing Cl. The Chemical shift of C-Cl was about 1eV.

Table S10. Binding Energies in eV of *rGO* functionalised by target molecules containing F obtained in present work and from refs 13 and 14.

Entry 1	Ar (1)	Target atom reference	C 1s C-F	F 1s	O 1s	Cl 2p	N 1s	S 2p _{3/2}
1	3-F(C ₆ H ₄) (1e)		285.4/286.6	686.8	532.4	200.0	399.3	167.9
2	4-F(C ₆ H ₄) (1f)		285.4/286.6	686.9	532.7	200.0	399.3	168.3
3	4-CF ₃ (C ₆ H ₄) (1g)		292.2 (+7.6)	687.8	532.7	200.2	399.2	168.2
4	3,5-(CF ₃) ₂ (C ₆ H ₃) (1h)		292.2 (+7.6)	687.6	532.7	200.0	399.0	167.9
5		Ar-CF ₃ ¹³	292.3					
6		Ar-F grafted by Diazonium ¹⁴	-	687.0 ^a				
7		Poly(vinyl trifluoroacetate) R-CF ₃ ¹⁵	292.3*	687.8 ^a				

^a F 1s value with C 1s calibration at 284.6 eV.

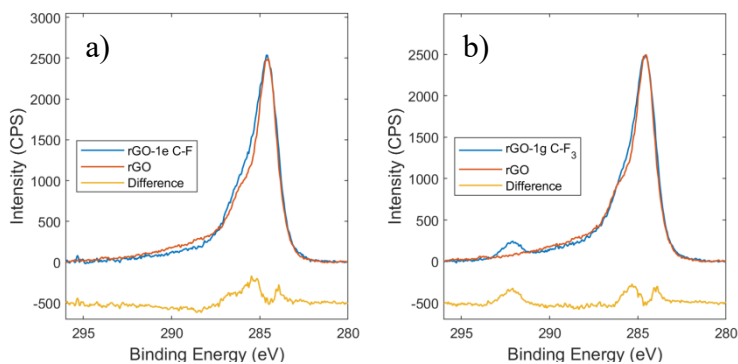


Figure S9. XPS C1s spectra of covalently grafted *rGO* by molecules containing F. The Chemical shift of C-F₃ was about 7.6 eV, while C-F present a +2 eV chemical shift.

Table S11. Binding Energies of *rGO* functionalised by target molecules containing Br.

Entry	Ar (1)	Target atom reference	C 1s C-Br	Br 3d	O 1s	Cl 2p	N 1s	S 2p _{3/2}
1	4-Br(C ₆ H ₄) (1i)		285.4 (+1.0)	70.1	532.6	200.0	399.3	168.1
2	3-Br(C ₆ H ₄) (1j)			70.0	532.9	200.0	399.5	168.0
3	2-Br(C ₆ H ₄) (1k)			70.1	532.7	200.0	399.3	168.0
4	2,4,6-Br ₃ (C ₆ H ₂) (1l)		285.6 (+1.2)	70.1	532.4	199.9	399.2	167.8
5		Ar-Br ¹⁶	-	70.2	-	-	-	-
6		Ar-Br ¹⁴		70.4				

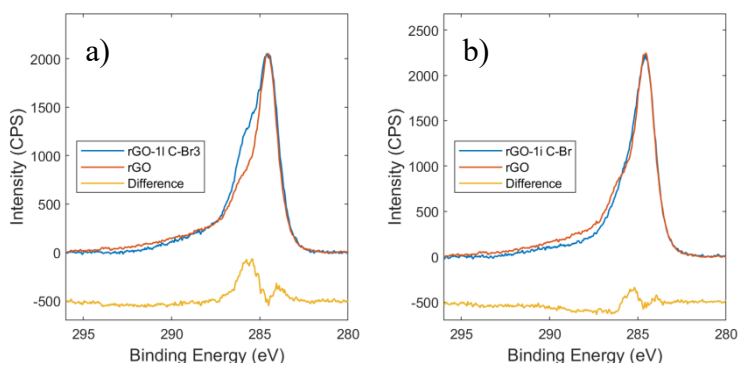
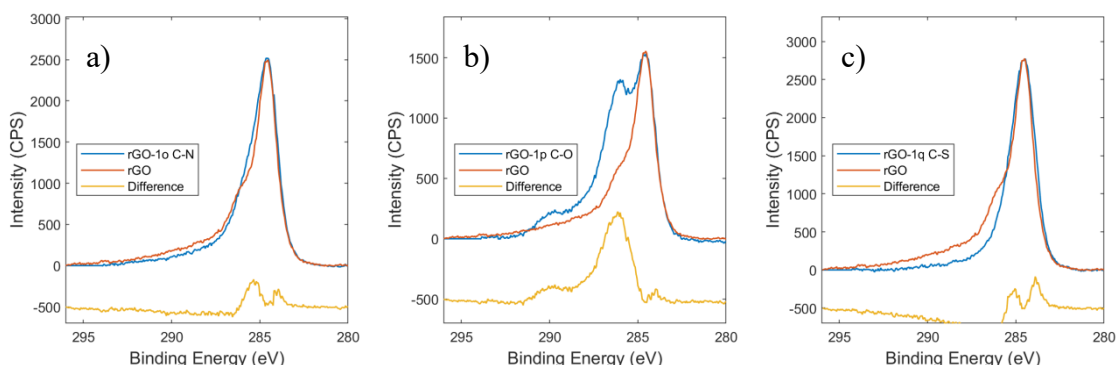
**Figure S10.** XPS C1s spectra of covalently grafted *rGO* by molecules containing Br. The Chemical shift of C-Br was about 1eV.

Table S12. Binding Energies of *rGO* functionalised by target molecules containing N and S.

Entry	Ar (1)	Target atom reference	C 1s	F 1s	O 1s	Cl 2p	N 1s	S 2p _{3/2} SO ₂	S 2p _{3/2} S-C
1	3-pyridyl (1o)		285.3 C-N	-	532.4	200.0	398.8	168.0	
2		P4VP ¹⁵ Aromatic N					399.3		
3	1p		C-S 286.0	-	532.9	199.9	399.2	168.0	163.9
4	1q			-	532.6	-	399.5	167.7	163.8
5		P3HT ¹⁷ Aromatic S							164.0

**Figure S11.** XPS C1s spectra of covalently grafted *rGO* by molecules containing N (a) and thiophenes (b,c). C-N group present a +0.9 eV chemical shift.**Table S13.** Binding Energies of *rGO* functionalised by target molecules containing I, and **1r-rGO** prepared by both path a (substitution of I on material **1m-rGO** via Suzuki coupling) and path b (via light promoted functionalisation with **1r** according to general procedure).

Entry	Ar (1)	Target atom reference	C 1s C-F	I 3d _{5/2}	F 1s	O 1s	Cl 2p	N 1s	S 2p _{3/2}
1	4-I(C ₆ H ₄) (1m)			620.6	-	532.7	199.9	399.5	168.3
2	2-I(C ₆ H ₄) (1n)			620.5	-	532.8	200.0	399.5	168.3
3	1r Path a		^a	620.3	688.3	532.7	-	399.5	168.2
4	1r Path b		292.2		687.6	532.7	199.8	399.0	168.1
5		Ar-I ¹⁸		620.6					

^a C 1s was superimposed to K 2p, identified by spin orbit split of 2.4 and presence of K 2s.

Raman characterization of the functionalized 1a-HOPG

In order to evaluate the effective covalent grafting Raman spectroscopy of Highly Oriented Pyrolytic Graphite (*HOPG*) was achieved, since *HOPG* presents extremely low residual defects and no D peak. Measurement was performed on clear area of *HOPG* surface, avoiding small crystals and edges occasionally present.

HOPG was cleaved by scotch tape and set in the same reactor used for *rGO* and *GO*, immersed for 24 h in a solution of **1a** in CH₃CN at room temperature. Control sample (**1a-HOPG** Dark) was done in the same condition, but with no LED light. Representative Raman spectra and optical microscope images of measured areas are reported in Figure S12.

Unfortunately, the results of Raman spectroscopy are indicative mainly for *HOPG*: as a matter of fact, a high amount of sp³ defects are already present on *rGO* and particularly on *GO*, so that the ID/IG ratios in these materials are close to unity. Moreover, in *GO* and *rGO* the grafting obtained by using aryl radicals from arylazocarboxylic tert-butyl esters in the presence of trifluoroacetic acid, as reported by Eigler¹⁹, showed a sp³ increase that corresponds to decrease in ID/IG (in highly defective materials the D band decreases in intensity respect to the G-band when the defects are increased, contrary to *HOPG* or pristine graphene, where the D-band increase with increasing defectivity) and to a broader 2D-band. In the above-mentioned paper was also demonstrated that aryl radical functionalization activated by acid environment is effective on both *GO* and pristine graphene. Therefore, the validation of covalent grafting obtained on *HOPG* can be extended for *GO* and *rGO*.

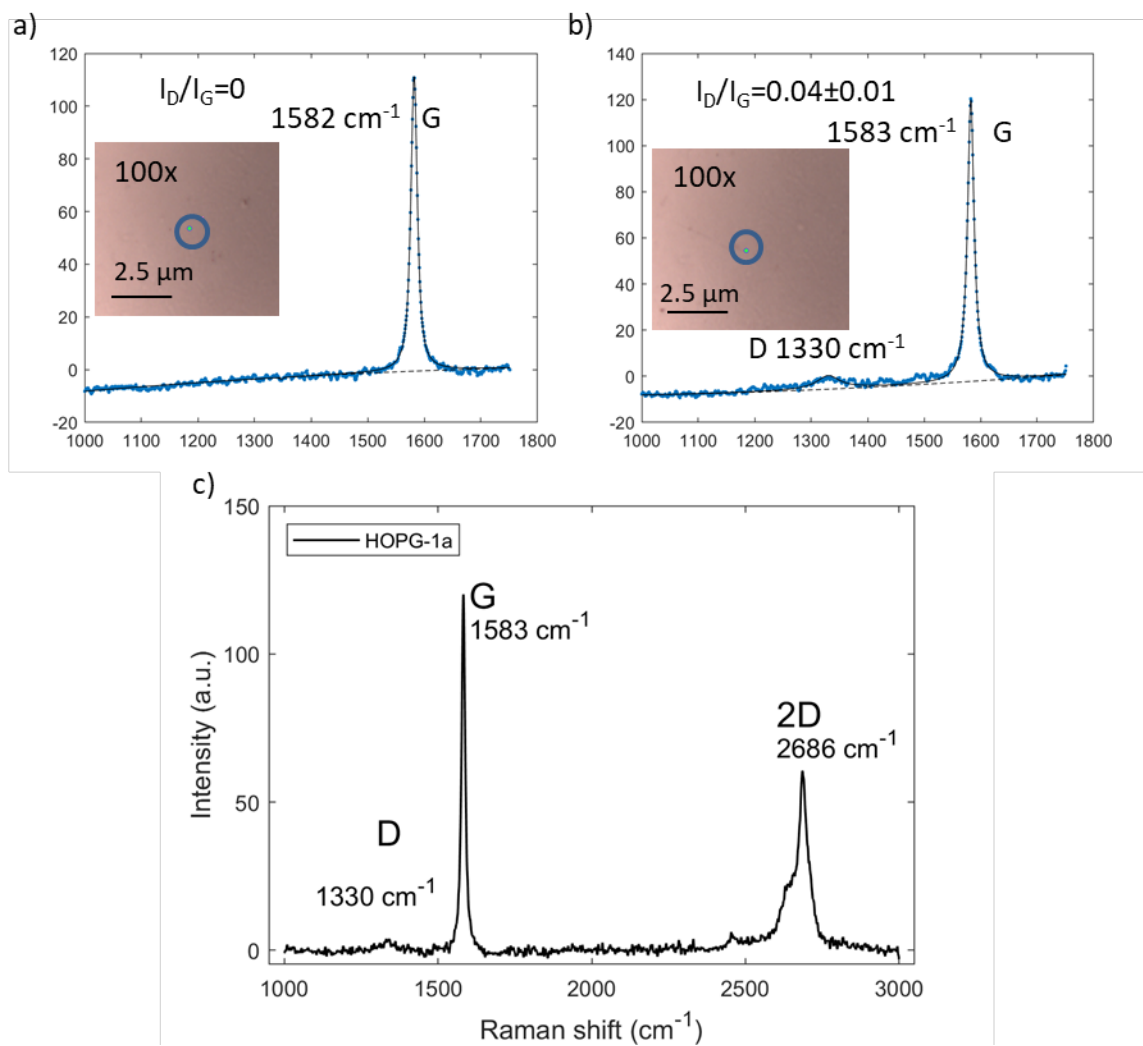
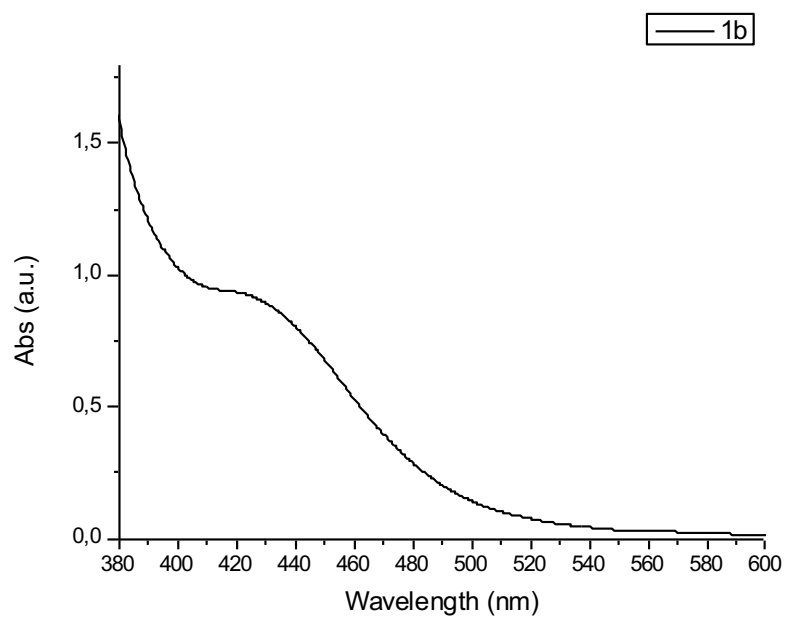
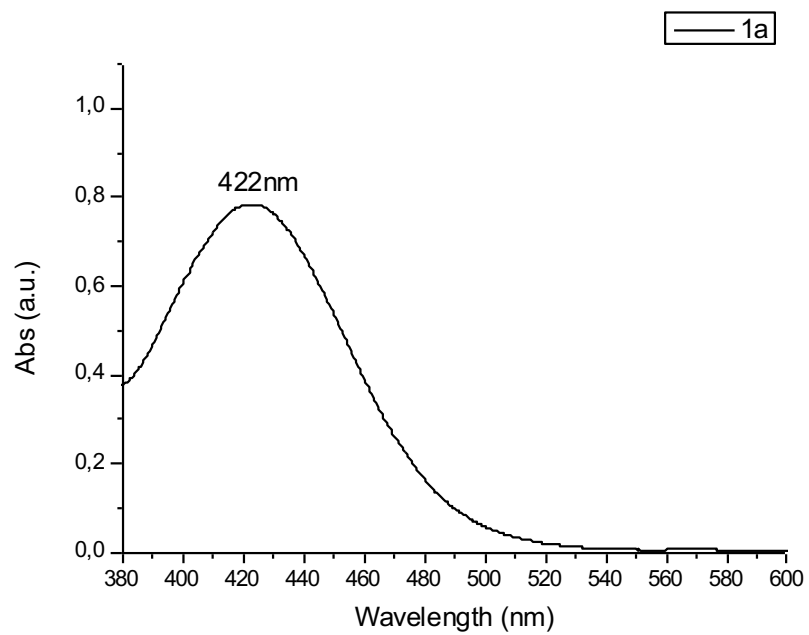
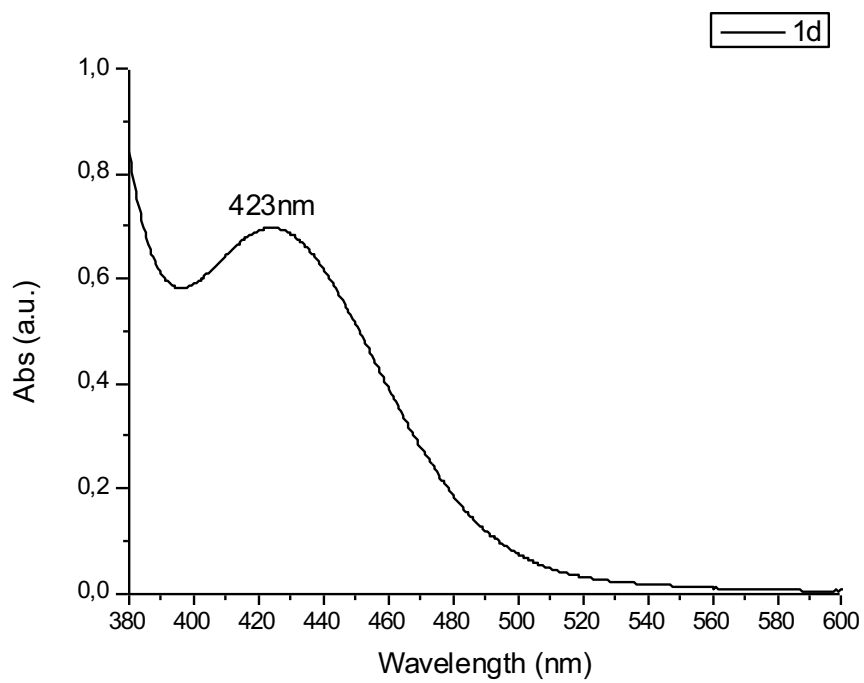
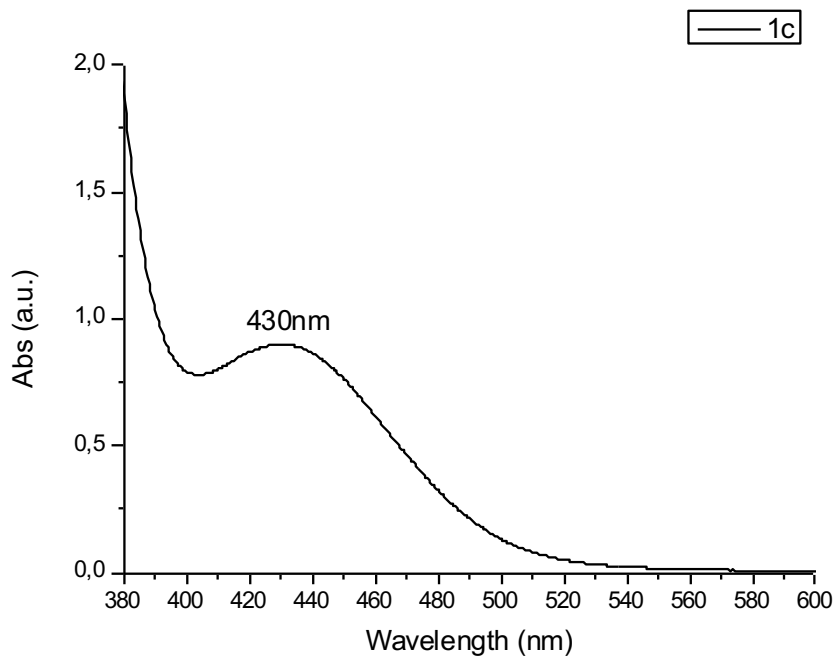
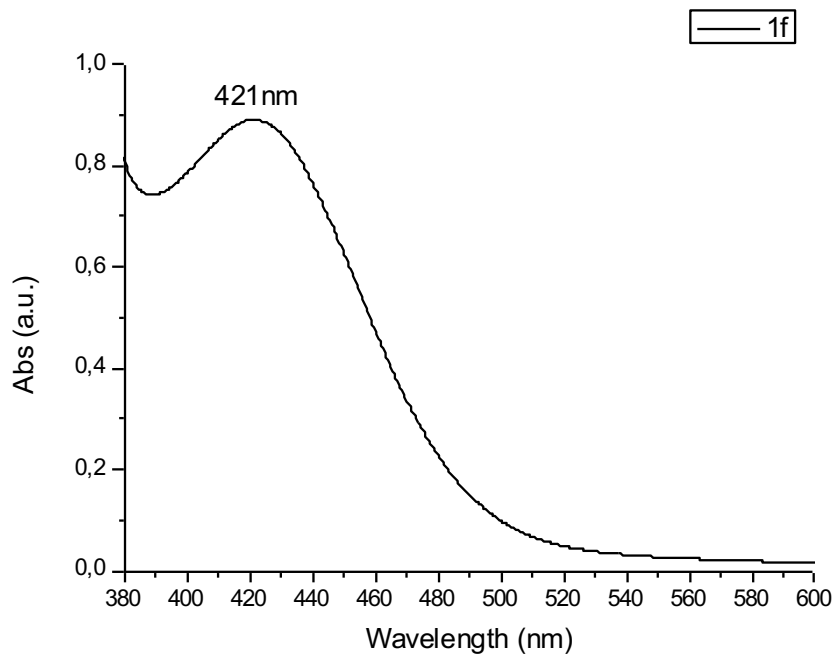
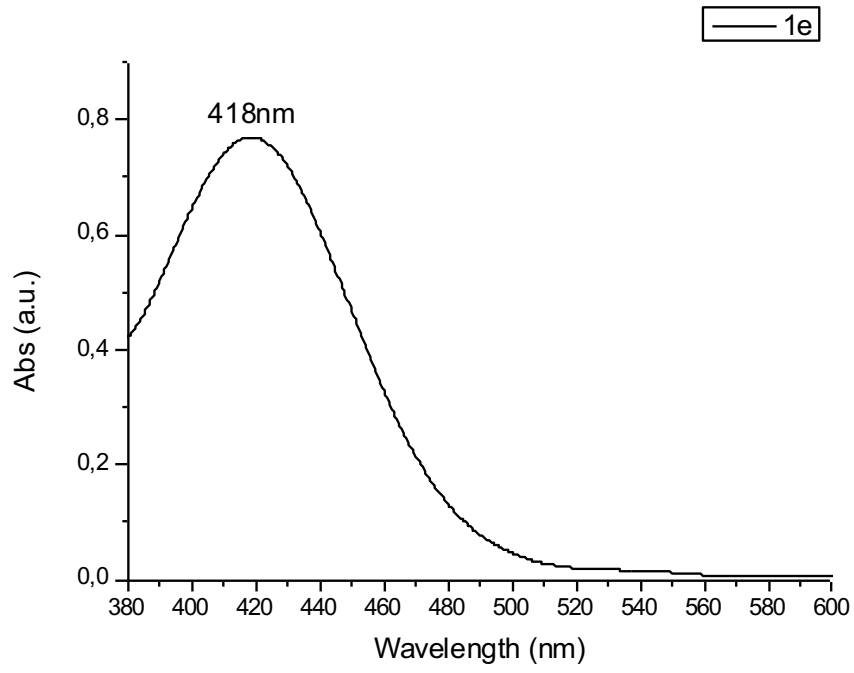


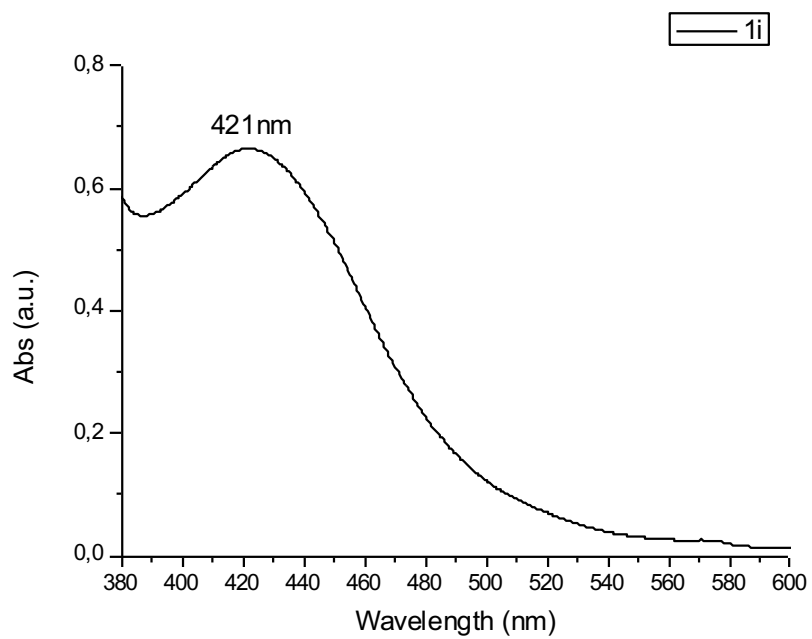
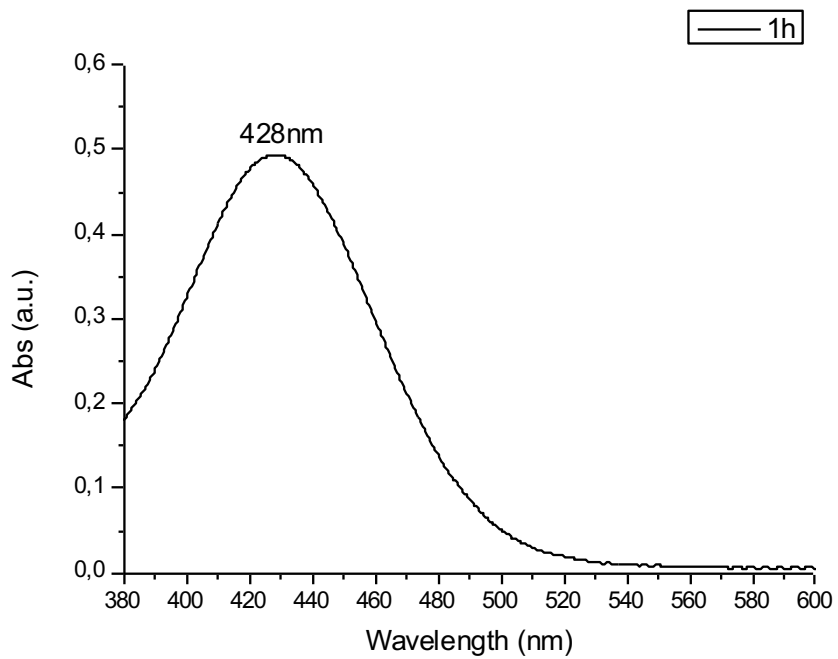
Figure S12. Raman spectrum and optical microscope image of probed area of (a) control sample and **1a-HOPG** Dark (b) sample after LED illumination **1a-HOPG**. (c) Full Raman spectrum of **1a-HOPG**.

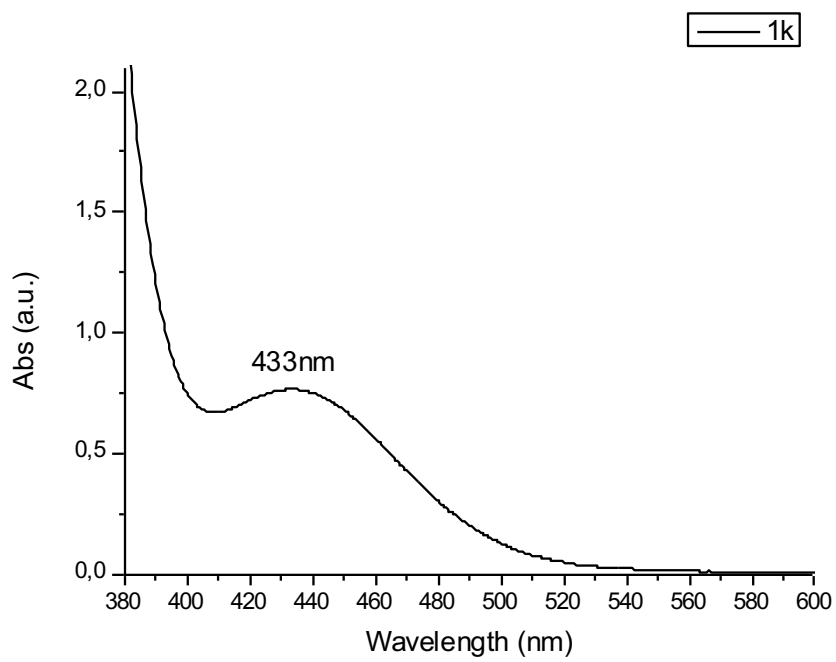
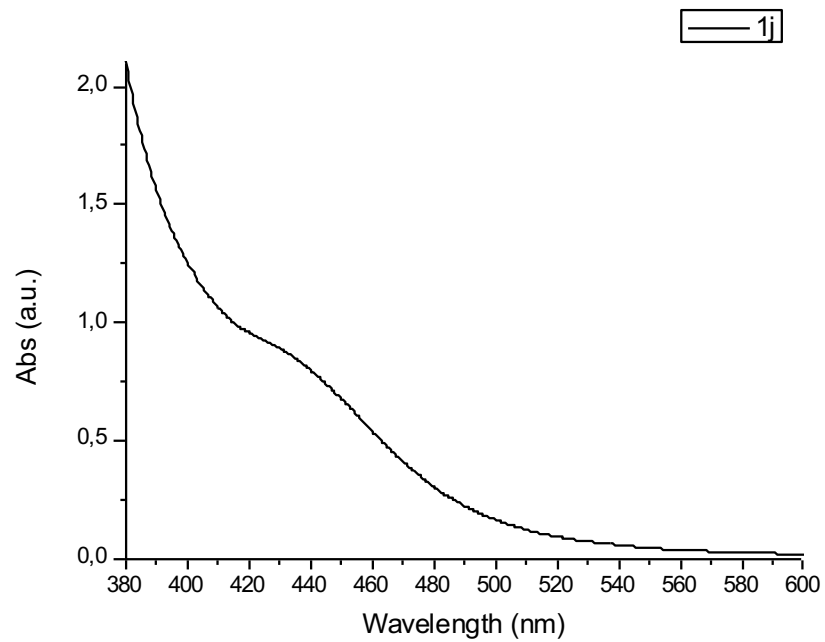
Absorption spectra [Arylazo mesylates (5 mM) H₂O:CH₃CN 1:1]

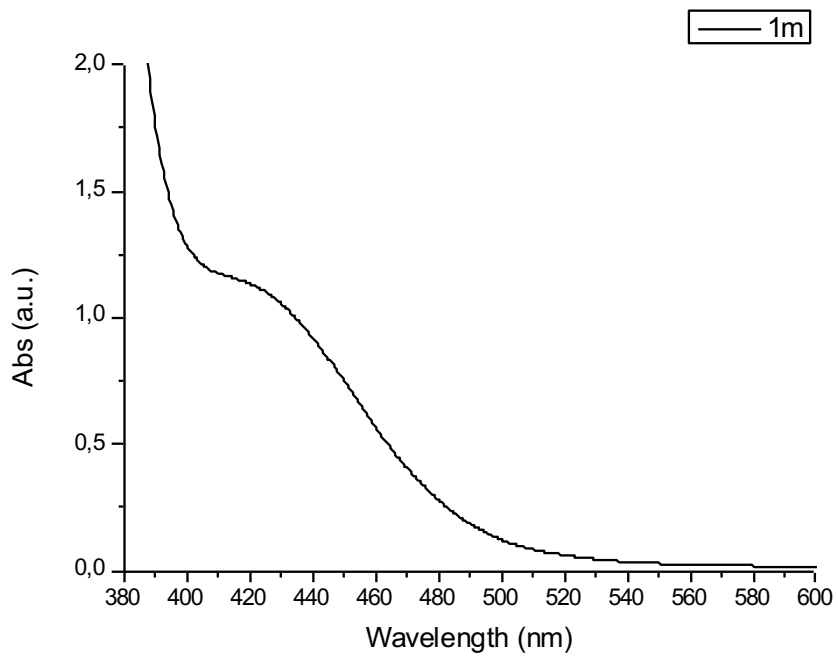
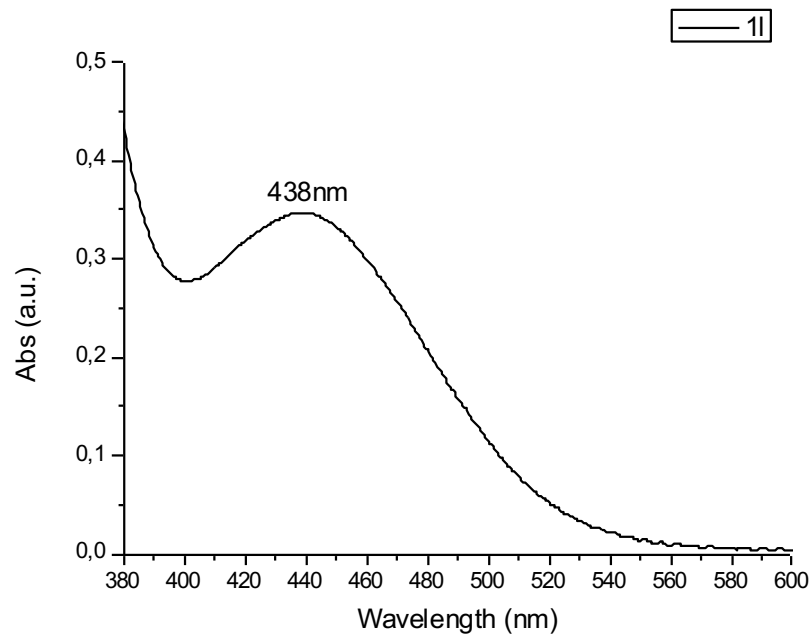


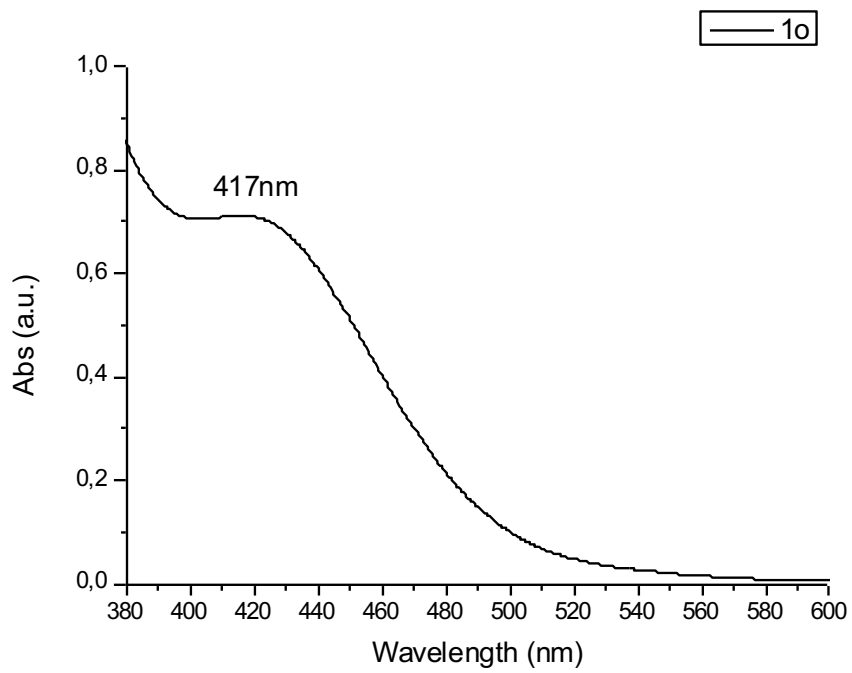
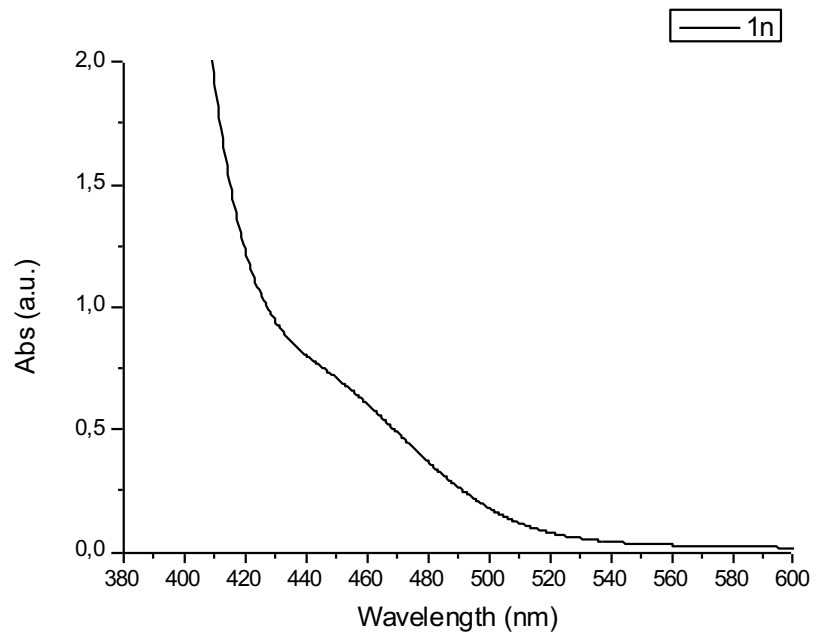


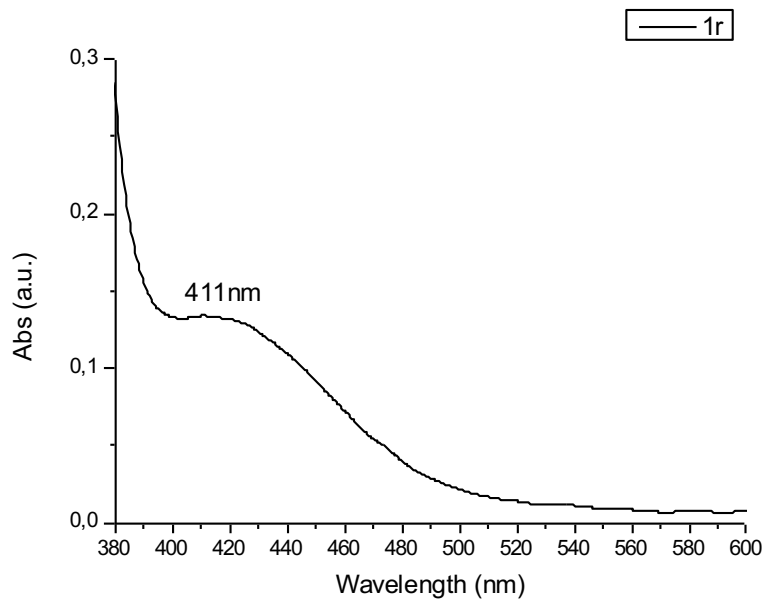
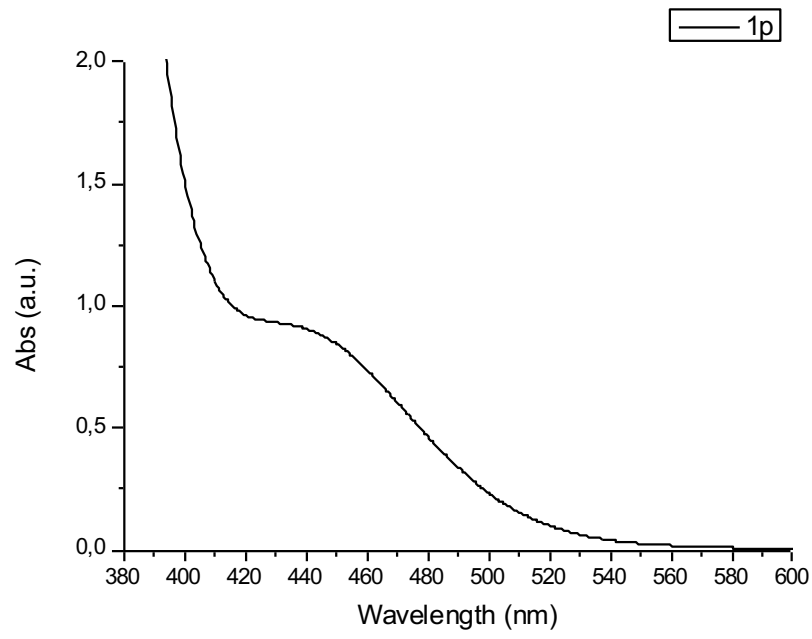






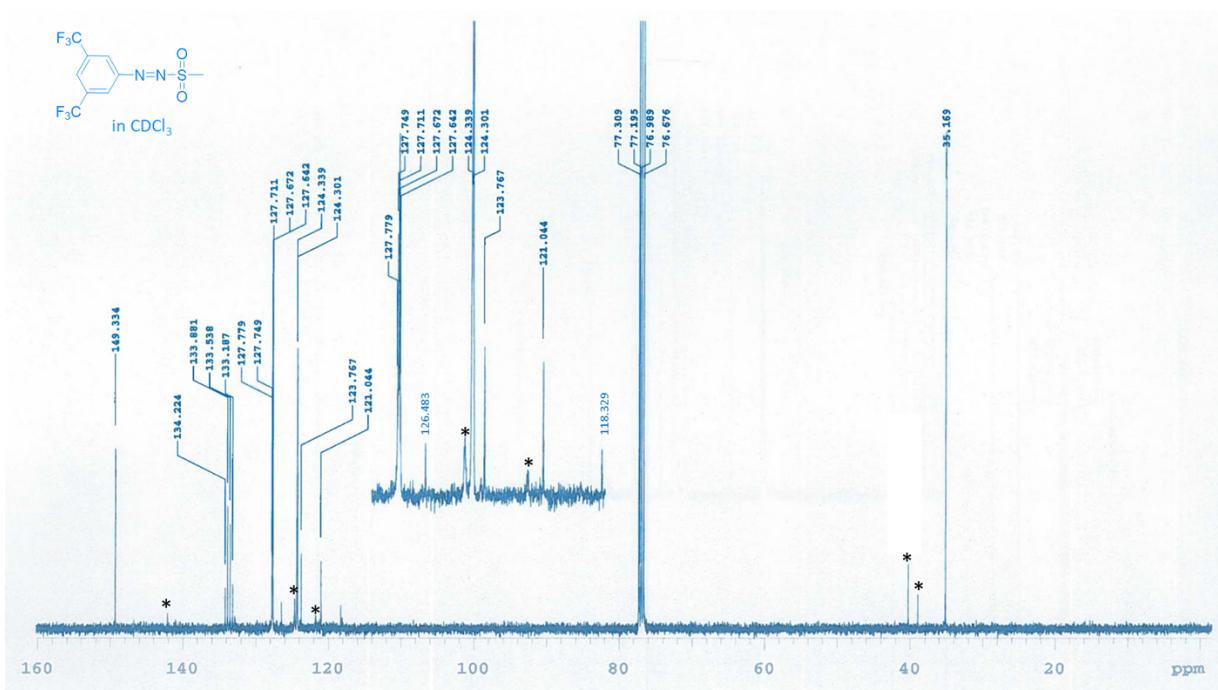
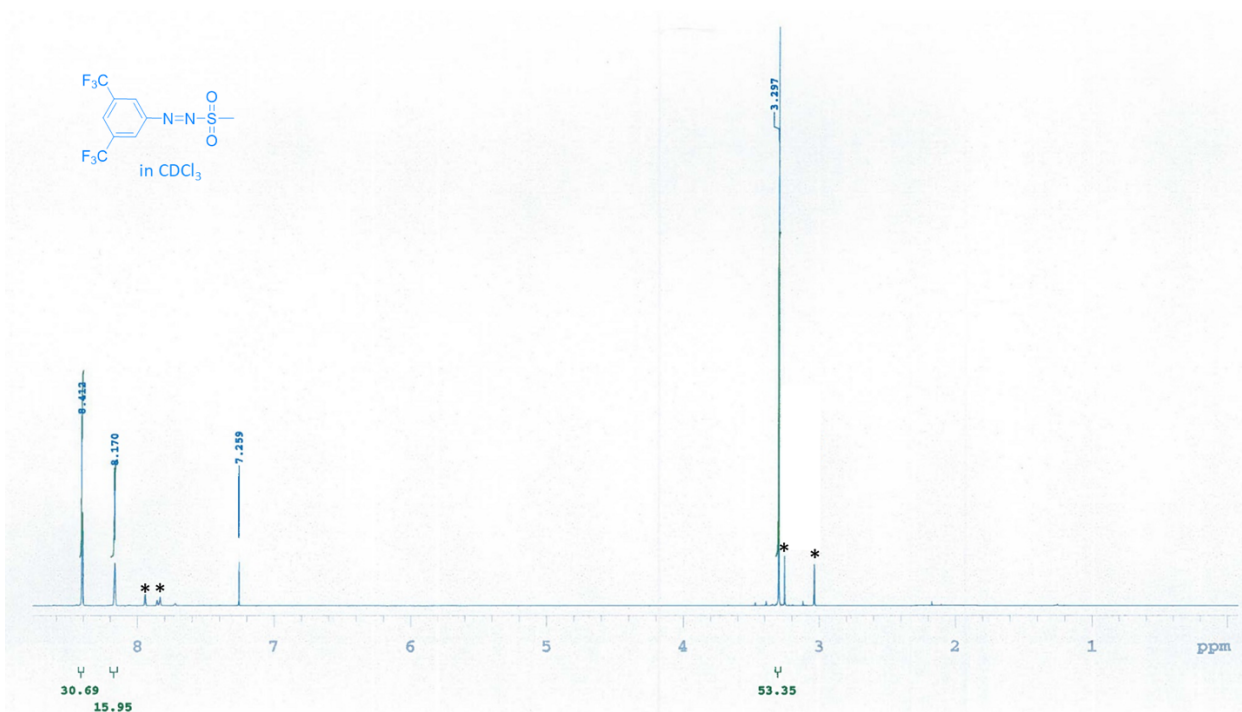


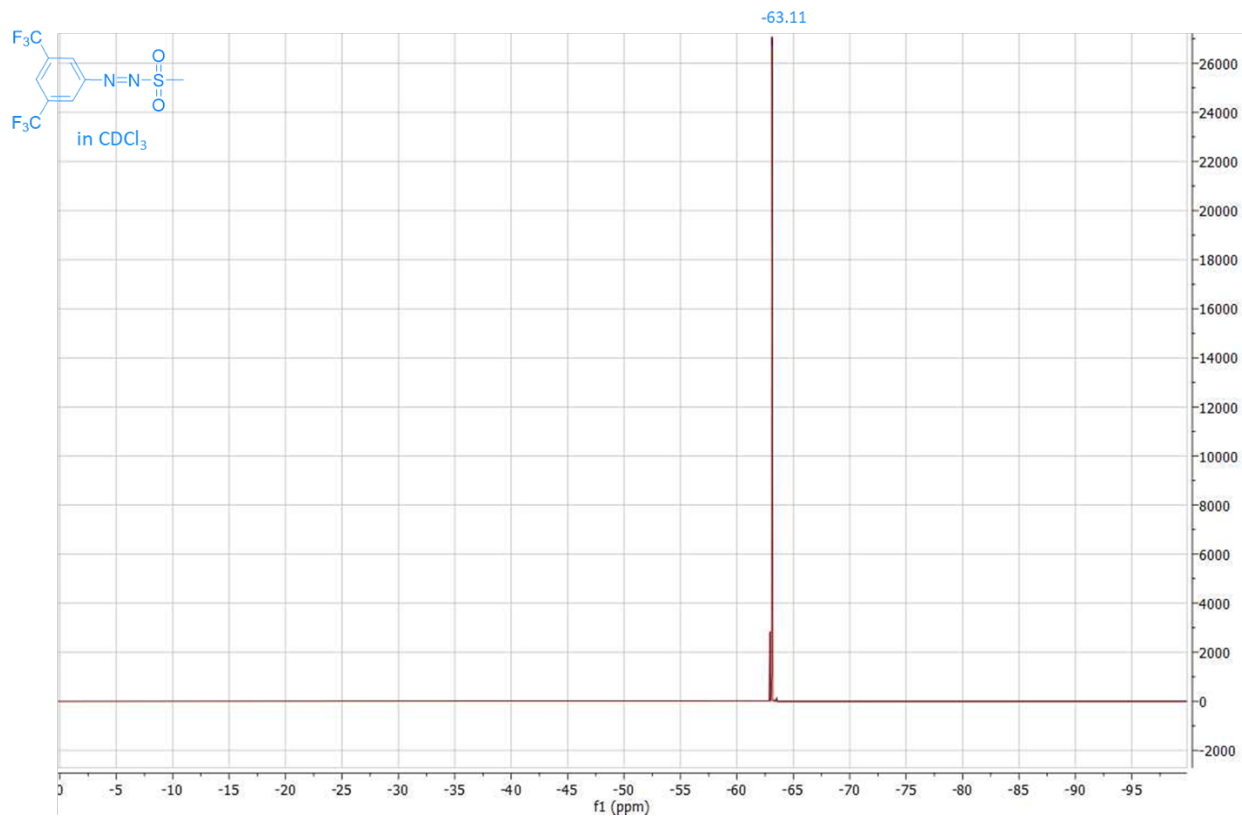




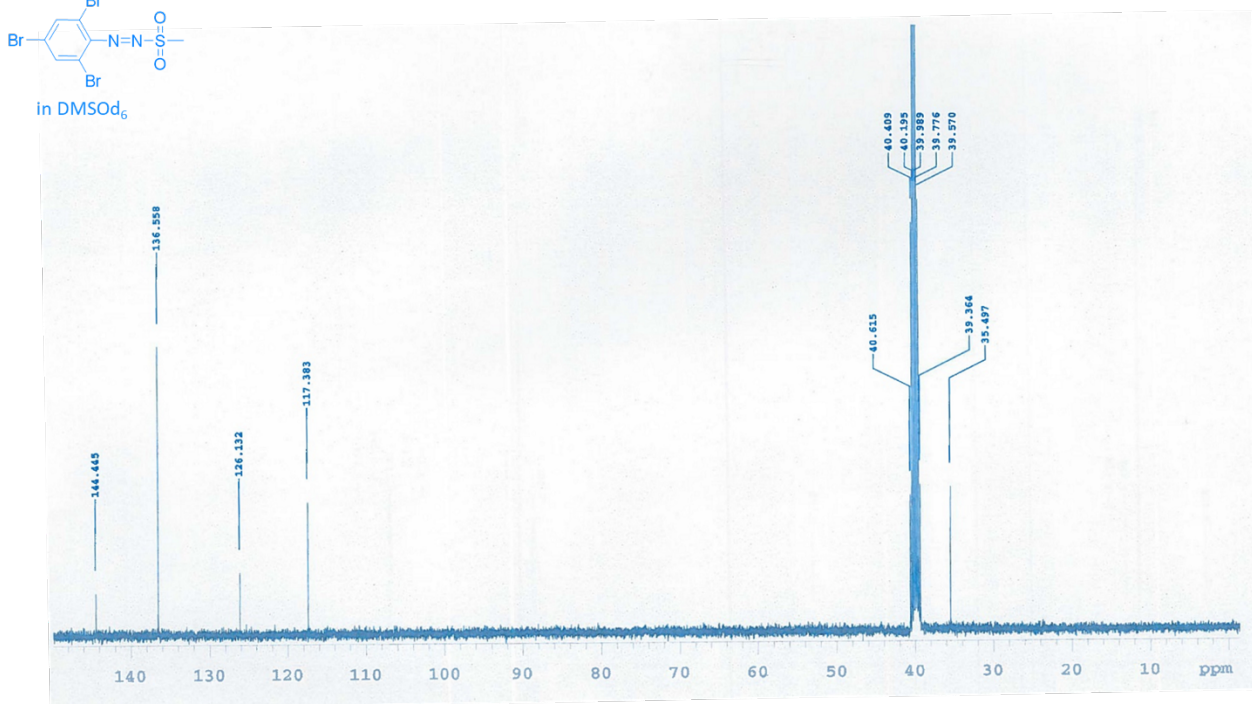
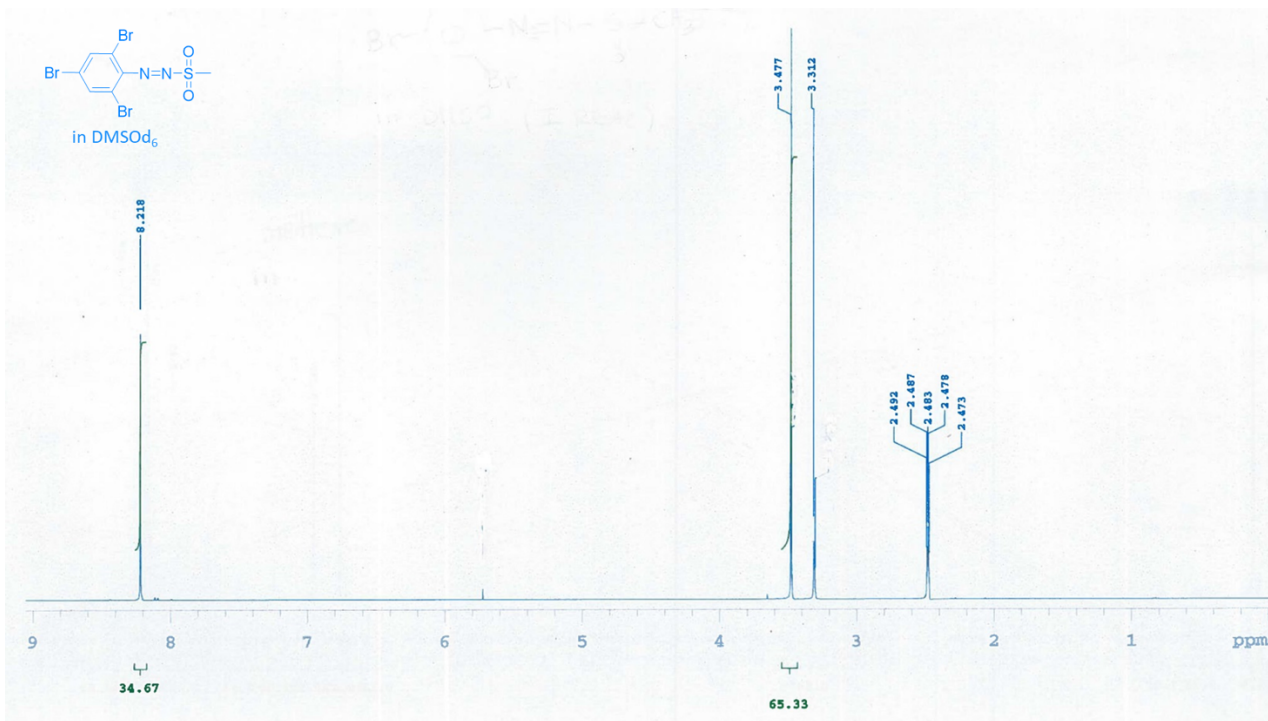
NMR Spectra of new compounds

Compound 1h

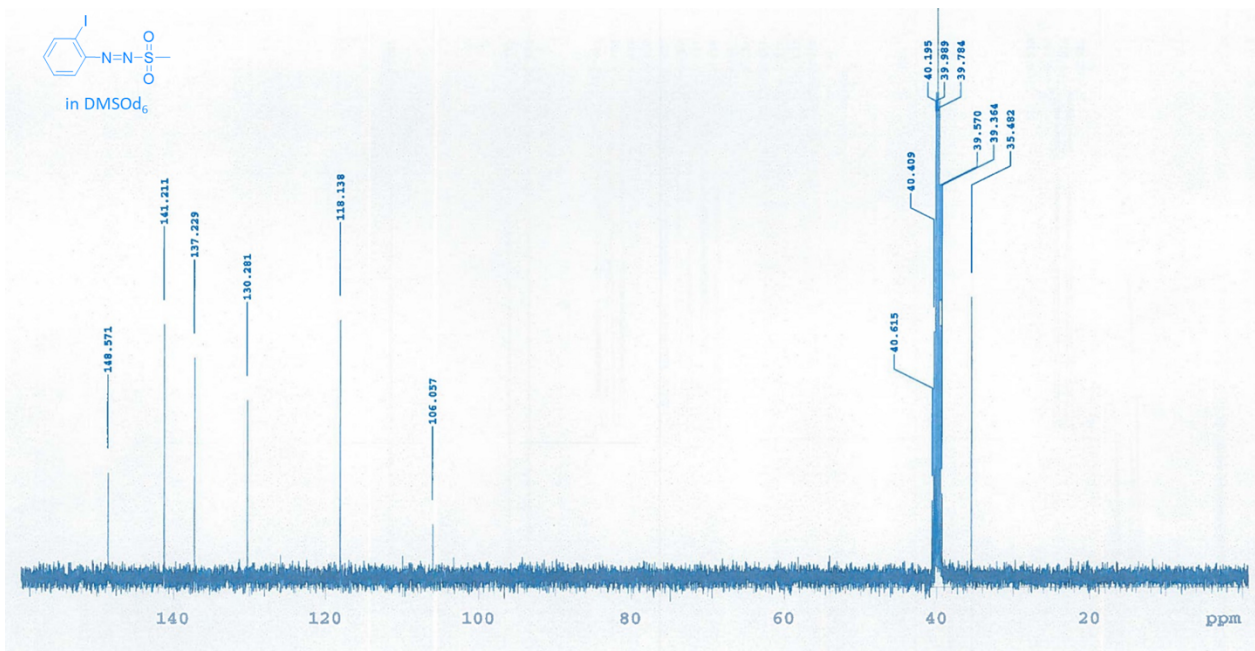
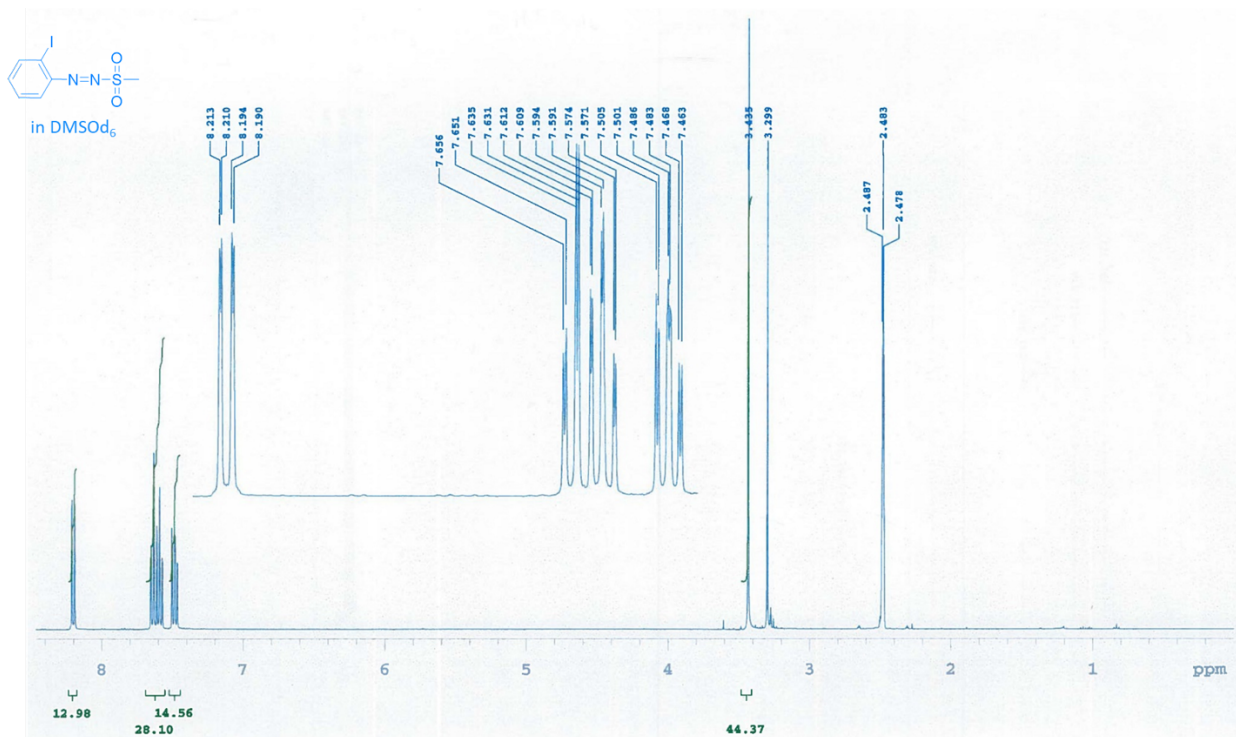




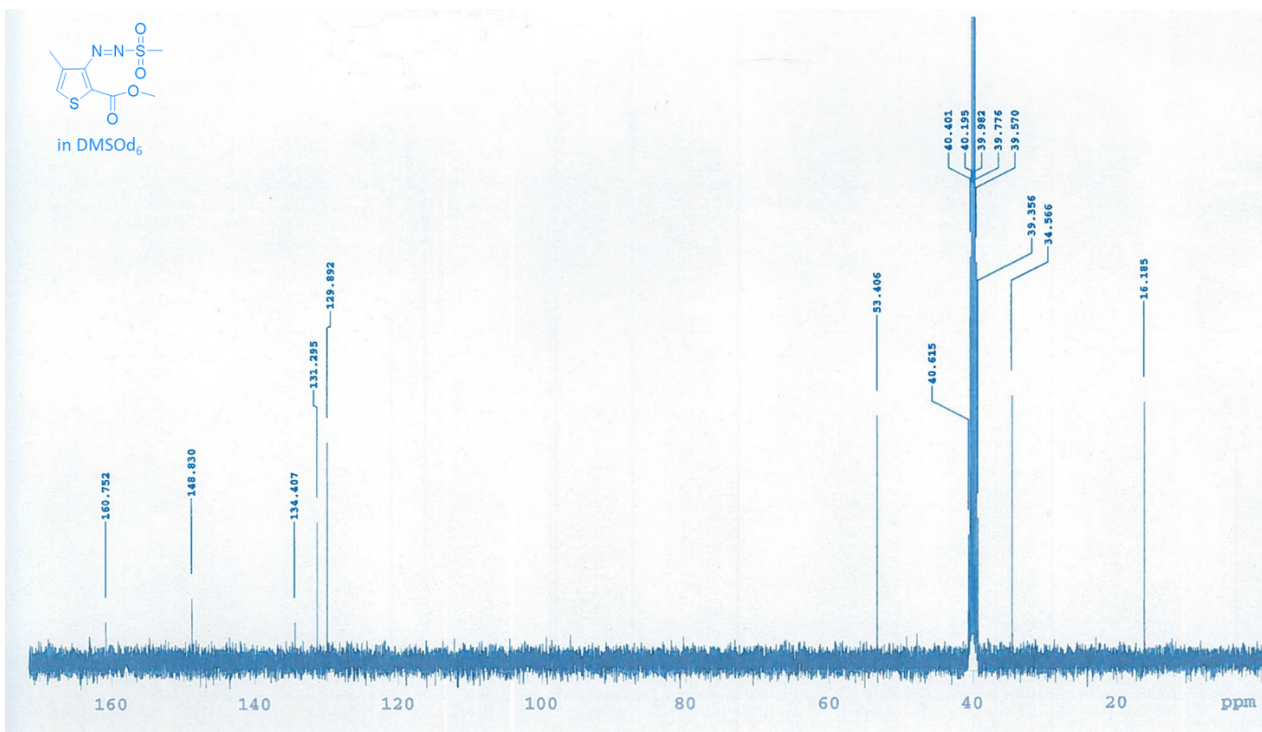
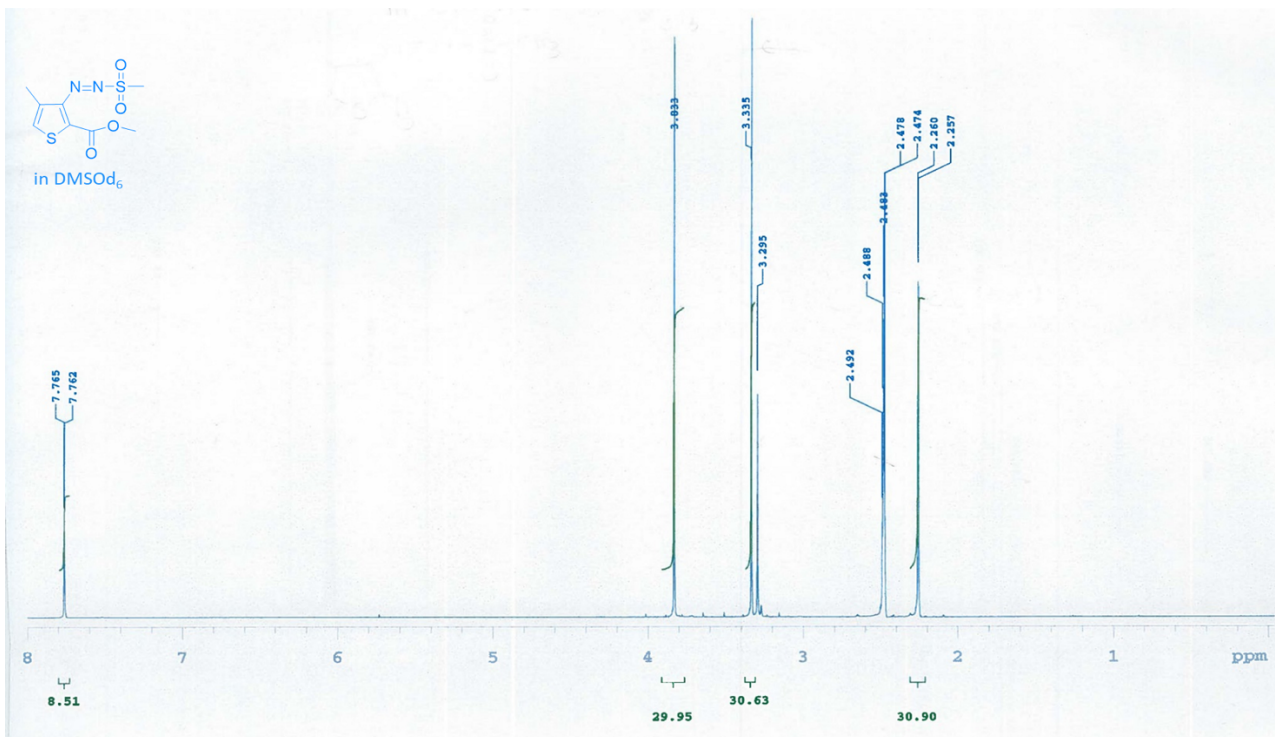
Compound 11



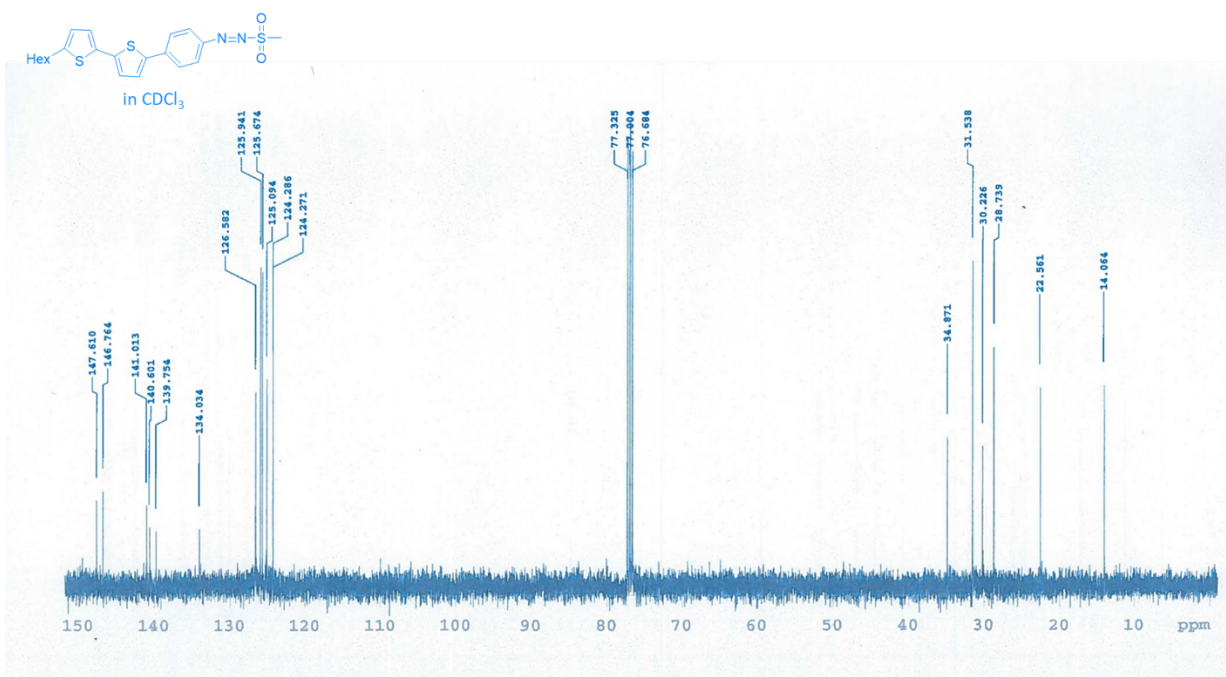
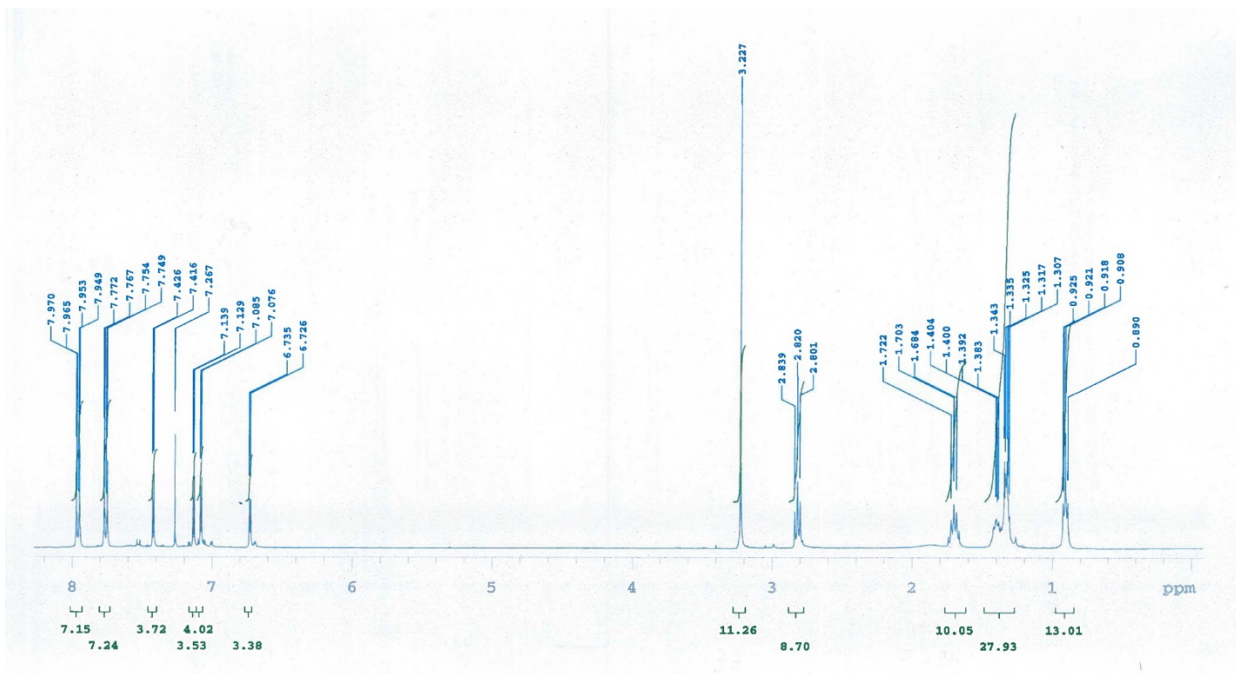
Compound 1n



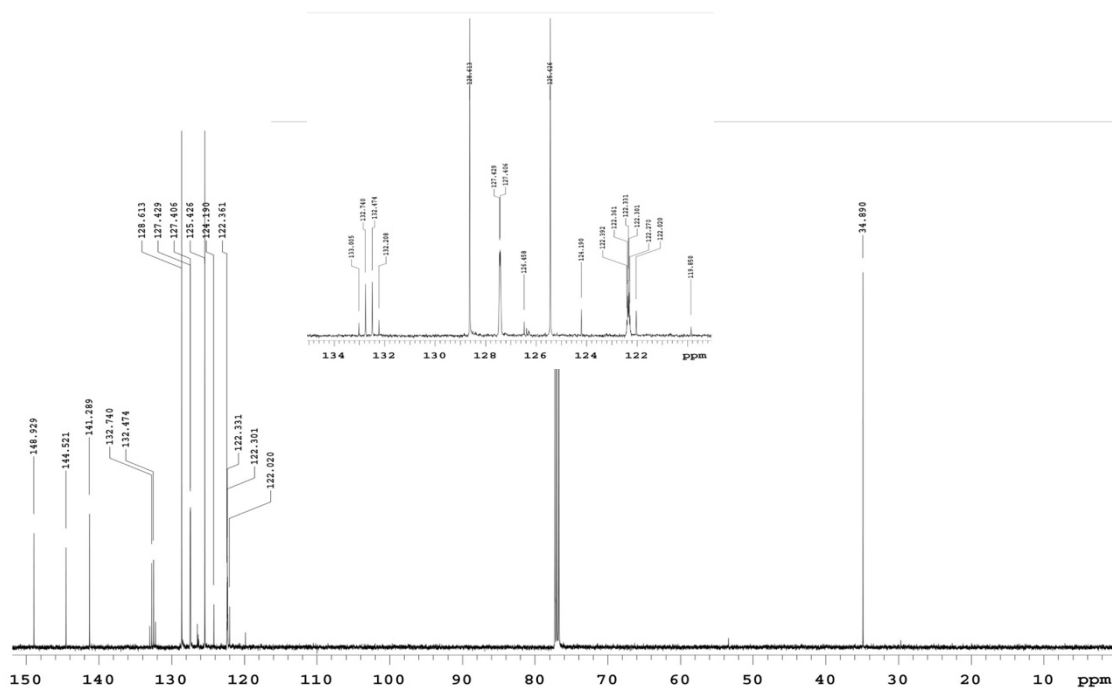
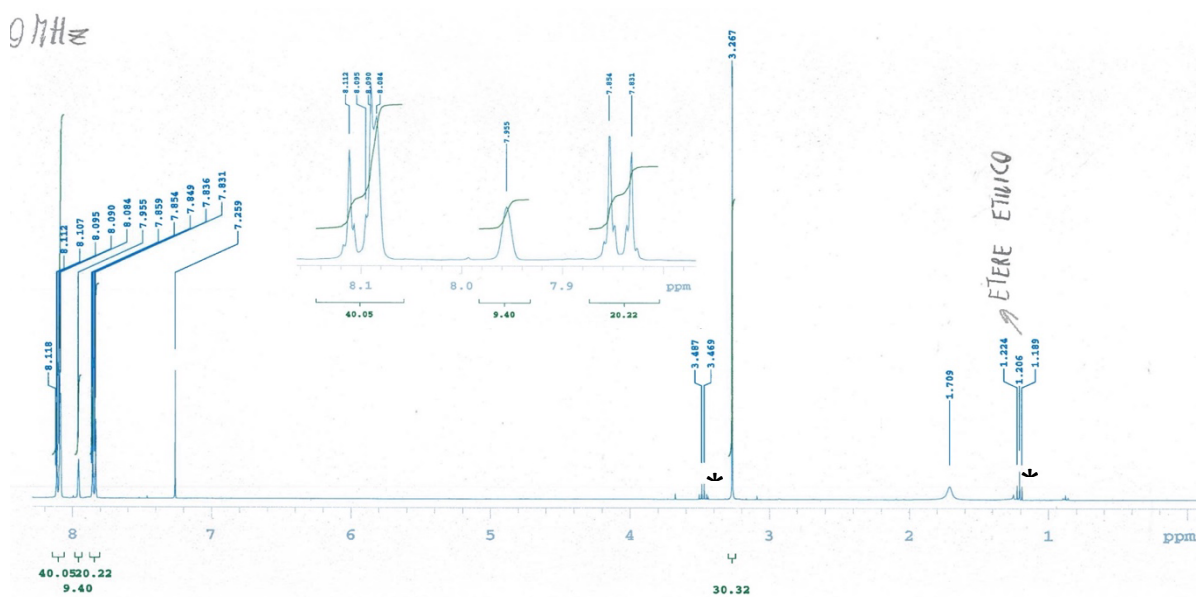
Compound 1p

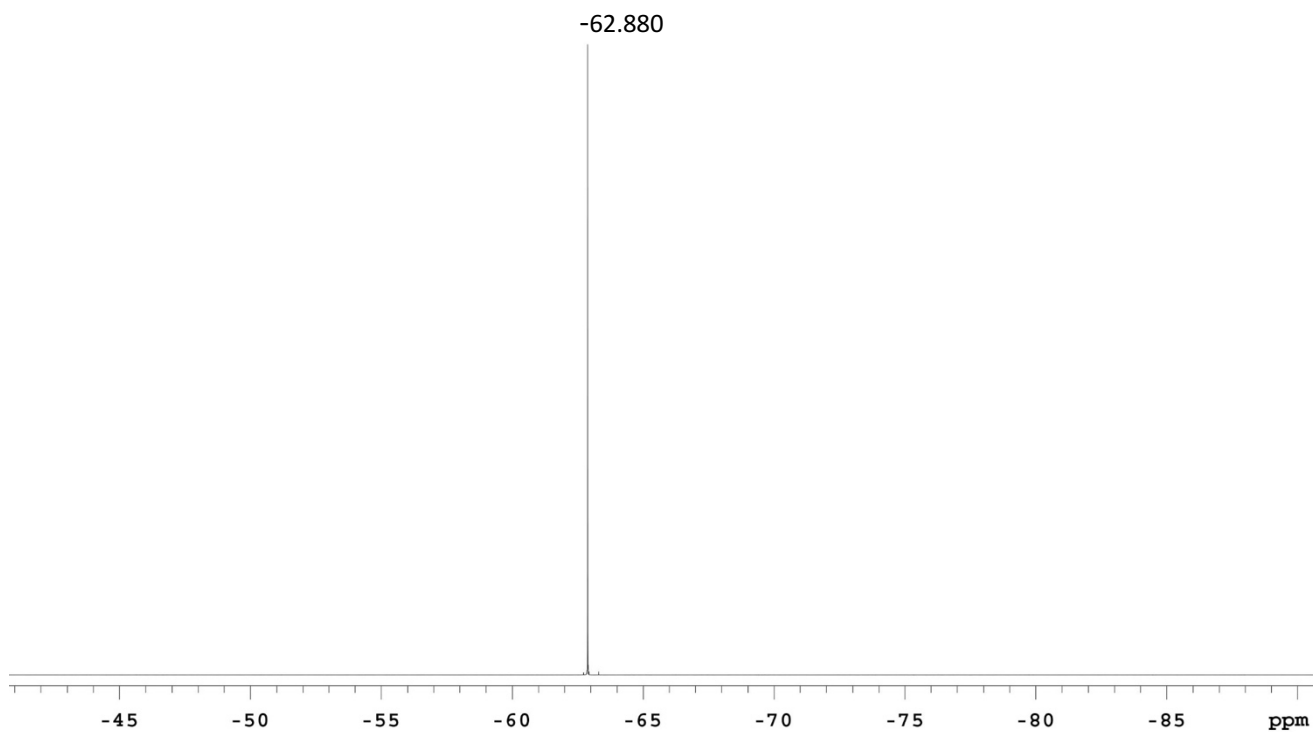
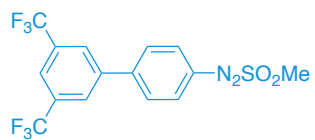


Compound 1q

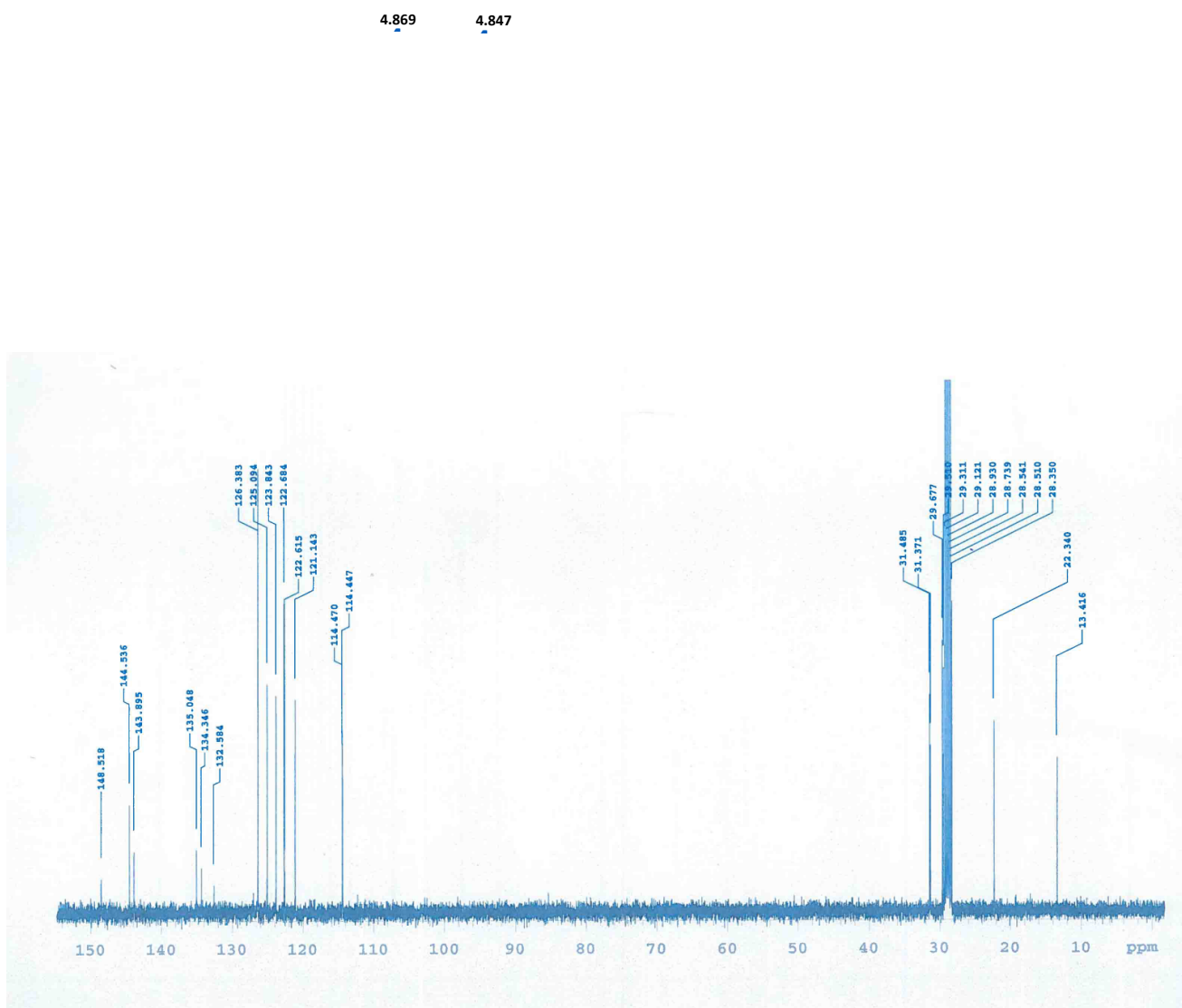


Compound 1r





Compound 2q (acetone-d₆)



References

- 1 Kovtun, A.; Jones, D.; Dell'Elce, S.; Liscio, A.; Palermo, V. Accurate chemical analysis of oxygenated graphene-based materials using X-ray photoelectron spectroscopy. *Carbon* **2019**, *143*, 268.
- 2 Larciprete, R.; Locovig, P.; Gardonio, S.; Baraldi, A.; Lizzit, S. Atomic Oxygen on Graphite: Chemical Characterization and Thermal Reduction. *J. Phys. Chem. C* **2012**, *116*, 9900.
- 3 Li, Y.; Xie, W.; Jiang, X. Mechanistic Study of a Photocatalyzed C-S Bond Formation Involving Alkyl/Aryl Thiosulfate. *Chem. Eur. J.* **2015**, *21*, 16059.
- 4 Crespi, S.; Protti, S.; Fagnoni, M. Wavelength Selective Generation of Aryl Radicals and Aryl Cations for Metal-Free Photoarylations. *J. Org. Chem.* **2016**, *81*, 9612.
- 5 Lian, C.; Yue, G.; Mao, J.; Liu, D.; Ding, Y.; Liu, Z.; Qiu, D.; Zhao, X.; Lu, K.; Fagnoni, M.; Protti, S. Visible-Light-Driven Synthesis of Arylstannanes from Arylazo Sulfones. *Org. Lett.* **2019**, *21*, 5187.
- 6 Blanka, L.; Fagnoni, M.; Protti, S.; Rueping, M. Visible Light-Promoted Formation of C-B and C-S Bonds under Metal- and Photocatalyst-Free Conditions. *Synthesis* **2019**, *51*, 1243.
- 7 Xu, Y.; Yang, X.; Fang, H. Additive- and Photocatalyst-Free Borylation of Arylazo Sulfones under Visible Light. *J. Org. Chem.* **2018**, *83*, 12831.
- 8 Amin, H. I. M.; Raviola, C.; Amin, A. A.; Mannucci, B.; Protti, S.; Fagnoni, M. Hydro/Deutero Deamination of Arylazo Sulfones under Metal- and (Photo)Catalyst-Free Conditions. *Molecules* **2019**, *24*, 2164.
- 9 Dato, F. M.; Sheikh, M.; Uhl, R. Z.; Schüller, A. W.; Steinkrüger, M.; Koch, P.; Neudörfl, J.-M.; Gütschow, M.; Goldfuss, B.; Pietsch, M. ω -Phthalimidoalkyl Aryl Ureas as Potent and Selective Inhibitors of Cholesterol Esterase. *ChemMedChem* **2018**, *13*, 1833.
- 10 Doring, M.; Uhlig, E.; Nefedov, V. I.; Salyn, I. V. Komplexbildung mit sulfonamidsubstituierten Thi-onoliganden. *Z. Anorg. Allg. Chem.* **1988**, *563*, 105.
- 11 Yoshida, T.; Sawada, S. The X-Ray Photoelectron Spectroscopy of o-Hydroxy Aromatic Azo Metal Complexes. *Bull. Chem. Soc. Jpn.* **1975**, *48*, 345.
- 12 Clark, D. T.; Kilcast, D.; Adams, D. B.; Musgrave, W. K. R. An ESCA study of the molecular core binding energies of the chlorobenzenes. *J. Electron Spectrosc. Relat. Phenom.* **1975**, *6*, 117.
- 13 Pandey, D.; Zemlyanov, D. Y.; Bevan, K.; Reifenberger, R. G.; Dirk, S. M.; Howell, S. W.; Wheeler, D. R. UHV STM I(V) and XPS Studies of Aryl Diazonium Molecules Assembled on Si(111). *Langmuir* **2007**, *23*, 4700.
- 14 Le Floch, F.; Matheron, M.; Vinet, F. Electrochemical grafting on SOI substrates using aryl diazonium salts. *J. Electroanal. Chem.* **2011**, *660*, 127.
- 15 SurfaceSpectra Ltd., *The XPS of Polymers Database*, (Eds.: G. Beamson, D. Briggs), Manchester, **2000**. (ISBN 0-9537848-4-3).
- 16 Rodríguez González, M. C.; Brown, A.; Eyley, S.; Thielemans W.; Mali, K. S.; De Feyter, S. Self-limiting covalent modification of carbon surfaces: diazonium chemistry with a twist. *Nanoscale* **2020**, *12*, 18782.
- 17 Lyon, J. E.; Cascio, A. J.; Beerbom, M. M.; Schlaf, R. Photoemission study of the poly(3-hexylthiophene)/Au interface. *Appl. Phys. Lett.* **2006**, *88*, 222109.
- 18 Bernard, M.-C.; Chausse, A.; Cabet-Deliry, E.; Chehimi, M. M.; Pinson, J.; Podvorica, F.; Vautrin-Ul, C. Organic Layers Bonded to Industrial, Coinage, and Noble Metals through Electrochemical Reduction of Aryldiazonium Salts. *Chem. Mater.* **2003**, *15*, 3450.
- 19 Halbig, C. E.; Lasch, R.; Krüll, J.; Pirzer, A. S.; Wang, Z.; Kirchhof, J. N.; Bolotin, K. I.; Heinrich, M. R.; Eigler, S. Selective Functionalization of Graphene at Defect-Activated Sites by Arylazocarboxylic tert-Butyl Esters. *Angew. Chem., Int. Ed.* **2019**, *58*, 3599.